Challenges in Replay Detection by TDLM in Post-Encoding Resting State

Simon Kern*[1,2,3,7], Juliane Nagel[1,2,3,7], Lennart Wittkuhn[8], Steffen Gais[6], Ray Dolan[4,5], Gordon Feld[1,2,3,7]

1 Clinical Psychology, Central Institute of Mental Health, Medical Faculty Mannheim, University of Heidelberg, Mannheim, Germany
2 Psychiatry and Psychotherapy, Central Institute of Mental Health, Medical Faculty Mannheim, University of Heidelberg, Mannheim, Germany
3 Addiction Behavior and Addiction Medicine, Central Institute of Mental Health, Medical Faculty Mannheim, University of Heidelberg, Mannheim, Germany
4 Max Planck UCL Centre for Computational Psychiatry and Ageing Research, London, UK
5 Wellcome Centre for Human Neuroimaging, University College London, London, UK
6 Institute of Medical Psychology and Behavioral Neurobiology, Eberhard-Karls-University Tübingen, Germany
7 Department of Psychology, Ruprecht Karl University of Heidelberg, Germany
8 Institute of Psychology, Universität Hamburg, Germany

Abstract:

We investigated, using temporally delayed linear modelling (TDLM) and magnetoencephalography (MEG), whether items associated with an underlying graph structure are replayed during a post-learning resting state. In these same data, we have previously provided evidence for replay during on-line (non-rest) memory retrieval. Despite successful decoding of brain activity during a localizer task, and contrary to predictions, we did not detect evidence for replay during a post-learning resting state. To better understand this, we performed a hybrid simulation analysis in which we inserted synthetic replay events into a control resting state recorded prior to the actual experiment. This simulation revealed that replay detection using our current pipeline requires extremely high replay densities to reach significance (>1 replay sequence per second, with “replay” defined as a sequence of reactivations within a certain time lag). Furthermore, when scaling the number of replay events with a behavioural measure we were unable to experimentally induce a strong correlation between sequenceness and this measure. We infer that even if replay was present at plausible rates in our resting state dataset we would lack statistical power to detect it with TDLM. We discuss ways for optimizing the analysis approach and how to find boundary conditions under which TDLM can be expected to detect replay successfully. We conclude that solving these methodological constraints is likely to be crucial to optimise measuring replay non-invasively using MEG in humans.

Introduction

Reactivation of memory traces during offline states is considered a core mechanism underlying memory consolidation. Memory reactivation has primarily been investigated in animal models, particularly in the context of hippocampal place cells (O'Keefe, 1976), wherein firing patterns that encode movements through a maze re-emerge later during rest periods (Pavlides & Winson, 1989), and their occurrence correlates with post-rest performance. Subsequently, memory reactivation has been linked to consolidation, i.e. the stabilization of long term memory traces (Born & Wilhelm, 2012; Feld & Born, 2017, 2020; Klinzing et al., 2019, Diekelmann & Born, 2010; Findlay et al., 2020; Foster, 2017; Wilson & McNaughton, 1994). Here, "memory reactivation" refers to the re-emergence of activation patterns in the absence of an eliciting sensory stimulus (Genzel et al., 2020). "Memory replay" on the other hand emphasizes a sequential ordering of reactivations, where replay patterns can follow a forward or backward trajectory (Diba & Buzsáki, 2007; Foster & Wilson, 2006). For example, backward replay is linked to reward processing during breaks in task performance (Ambrose et al., 2016). An additional feature of replay is its time-compression, such that its time-course is much faster than the temporal evolution of the original encoded activity (Nádasdy et al., 1999).

Replay has been confirmed by cellular recordings in a large variety of mammalian model organisms (Hoffman & McNaughton, 2002; Lee & Wilson, 2002; Pavlides & Winson, 1989). However, human replay studies are relatively few, as most methods rely on invasive methods such as intracranial electroencephalography (iEEG) or stereotactic electrodes (Axmacher et al., 2008; Engel et al., 2005; Staresina et al., 2012, 2015; Zhang et al., 2015). As these methods are only applied under restricted clinical circumstances, such as during pre-operative neurosurgical assessments, this limits opportunities to investigate human replay. Therefore, efforts to derive novel methods to investigate human replay non-invasively are needed.

Non-invasive neuroimaging techniques suffer a trade-off (Hall et al., 2014) – either their spatial precision is high but their temporal precision is lacking, as with functional magnetic resonance imaging (fMRI), or vice versa as with magneto- or electroencephalography (MEG/EEG). This has motivated the development of sophisticated analytical approaches to overcome these limitations. While measuring faster sequences is possible with fMRI (Schuck & Niv, 2019; Wittkuhn et al., 2024; Wittkuhn & Schuck, 2021), most recent human replay research has focused on MEG or EEG based analysis (Y. Liu et al., 2022).

Using advances in brain decoding, that also exploit the temporal precision of MEG, one approach to quantifying replay involves examining lag differences between individually decoded reactivation events (Kurth-Nelson et al., 2016; Y. Liu, Dolan, et al., 2021), a method referred to as

“Temporally delayed linear modelling” (TDLM). In essence, by computing a “sequenceness” score, the method quantifies whether a sequence of decoded brain activity appears more often than expected by chance. Using this approach, a series of studies have provided evidence that individual states are replayed in sequence not only during rest (Eldar et al., 2020; Q. Huang et al., 2024; Y. Liu et al., 2019; Nour et al., 2021, 2023; Yu et al., 2023) but also during in the context of active cognition including planning/decision making (Eldar et al., 2020; W. Huang et al., 2020; Kurth-Nelson et al., 2016; McFadyen et al., 2023; Schwartenbeck et al., 2023; Seow et al., 2024; Wimmer et al., 2023; Wise et al., 2021), memory retrieval (Huang & Luo, 2023; Kern et al., 2024; Wimmer et al., 2020) and following reward reception (Liu, Mattar, et al., 2021).

Relevant to the current study, off-line replay of task-relevant sequences has been reported across several studies. Liu et al. (2019) reported on participants who first learned a rule based mapping of items, followed by a 5-minute resting state activity recording, prior to completion of a subsequent task. In one study iteration, value learning was applied to one of two sequences of sensory items. During the resting session, states were replayed at around 40-60 milliseconds time lag, in a predominantly forward or backward direction, depending on whether a specific sequence was rewarded or not. Eldar et al. (2020), found sequenceness during resting state was associated with lessened flexibility to subsequent changes in value-location pairings, consistent with supporting model-free decision-making. In the latter study, backward replay was reported during rest at a 180-millisecond time lag, albeit using a cross-correlation approach, a predecessor method to TDLM. Nour et al. (2021) found attenuated rest period replay at a time lag of 40-50 milliseconds in patients with schizophrenia compared to healthy controls. In the same data, Nour et al. (2023) found that patients showed reduced coupling of replay to default-mode-network-activation, and this impairment correlated with memory retention. Yu et al., (2023) used EEG recordings in a sequence-learning task in participants with trait anxiety and found that individuals with higher trait anxiety showed reduced reverse replay of reward sequences during a resting state. Finally, Huang et al., (2024), used simultaneous EEG-fMRI to examine the spatial and temporal dynamics of memory replay in humans and showed that during mental simulation replay events were associated with activation in the hippocampus and medial prefrontal cortex.

In the current study, our focus was on the consolidation of graph-based task structures during resting state as captured in MEG data. Previous research indicates that recently acquired mnemonic memories are replayed in subsequent rest or sleep sessions (Humiston et al., 2019; Schapiro et al., 2018; Schreiner et al., 2021; Tambini et al., 2010; Wamsley, 2022), with replay density slowly decreasing over a time window of two hours (Eschenko et al., 2008a) . Additionally, it is reported that replay at rest and during sleep preferentially consolidates items based on properties such as encoded strength (Drosopoulos et al., 2007; Huelin Gorriz et al., 2023; Schapiro et al., 2018)

or graph node properties (Feld et al., 2022). Therefore, in our study, we employed criterion learning to 80% correct retrieval on a graph network, a criterion similar to the performance participants achieved on a similar graph-based task which showed a sleep benefit (Feld et al., 2022). We assumed this would achieve a level of memory acquisition that would engender subsequent sequence replay, as it allowed for further memory improvement, which we inferred, would depend on subsequent replay. Criterion learning is a standard practice in studies on sleep-dependent memory consolidation (e.g. Feld et al., 2013; Galer et al., 2015; Payne et al., 2012; Rasch et al., 2006).

We acknowledge here that previous studies using TDLM focused primarily on structural inference and decision making and not on mnemonic learning (Eldar et al., 2020; Y. Liu et al., 2019; Y. Liu, Mattar, et al., 2021; Nour et al., 2021, 2023). Nevertheless, we considered it likely that there would also be replay after mnemonic learning (Buhry et al., 2011; Findlay et al., 2020; Zhou et al., 2024) and, if present, this would be amenable to quantification using TDLM. Despite this prediction, we did not find replay evidence in our post-learning resting state session. To further investigate this lack of sequenceness we conducted a second study wherein we simulated replay by inserting, at varying densities, neural events taken from the localizer data, into a control resting state recorded before any stimulus exposure. This simulation allowed us within our pipeline, to quantify a lower bound of replay density necessary to detect replay. Additionally, to simulate a previously demonstrated association of replay and performance (e.g. Schapiro et al., 2018; Wimmer et al., 2020), we scaled simulated densities by participant's performance. Finally, we discuss existing uncertainties regarding parameter choices and possible resulting confounders when using TDLM as well as suggesting ways to improve the robustness of the method.

Results Study I: Resting State Analysis

In study I, participants were first placed in an MEG scanner for an 8-minute resting state measurement (see Figure 1 for an overview of the procedure). Next, while subjects remained in the scanner, we performed a localizer task on which a classifier was trained. Participants then learned triplets of associated items according to a graph structure, up to a memory performance criterion of 80% (see Methods for details). Finally, participants were asked to remain in the scanner for a further 8-minute resting state measurement after which we tested memory retrieval. Mean learning performance of ~82% indicated that the applied criterion learning was successful.

We found no evidence for sequenceness that reflected task structure in the post-task resting state. Behavioural results indicated that the experimental manipulation worked as intended, i.e., participants learned the graph to criterion, without overlearning which might have obviated the occurrence of replay (see Figure 2). Additionally, we tested for a correlation of memory performance and sequenceness strength, as group-level sequenceness thresholds might be too conservative alone, but found none. Note that data from the retrieval stage were published elsewhere (Kern et al., 2024). The study and analysis were preregistered at aspredicted.org (https://aspredicted.org/kx9xh.pdf, #68915).

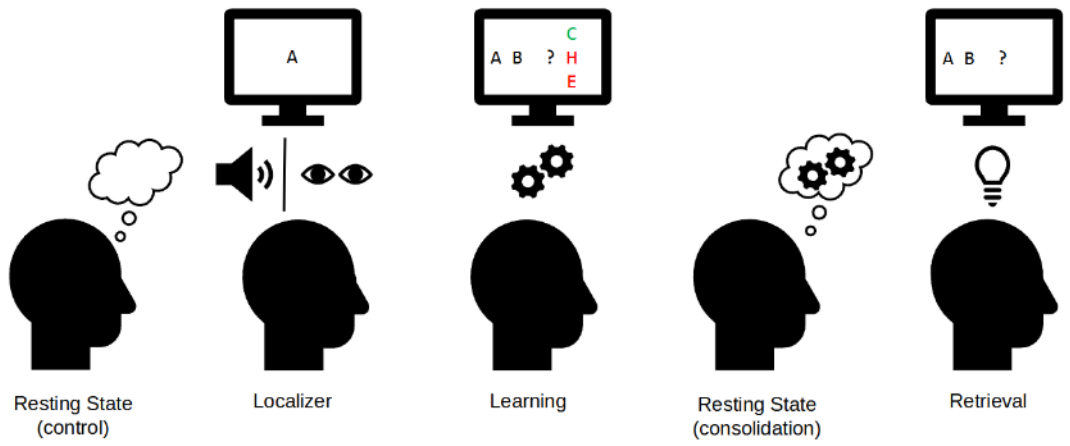

Figure 1 Experimental procedure in the MEG. Control: Eight minutes of resting state activity were recorded before participants encountered any stimuli. Localizer task: Next, the ten individual items were repeatedly presented to participants auditorily and visually to extract multisensory activity patterns. Learning: Participants learned triplets of the ten items pseudo-randomly generated based on an underlying graph, by performing a three-alternatives-forced-choice. Participants were unaware of the graph layout. Consolidation: Eight minutes of resting state activity were recorded. Retrieval:

Participants' recall was tested by cueing triplets from the graph. The letters in the pictograms are placeholders for individual images. Figure and caption adapted from Kern et al., (2024). For details, see Supplement Figure 1.

Behavioural results

All thirty participants, except one, learned the graph consisting of images to a criterion of 80%. After a consolidation resting state, a marginal increase in performance was observed (76% to 82% accuracy, t=-2.053, p=0.053, effect size r=0.22 Figure 2A), but note that this must not necessarily be attributed to consolidation, as the last block also included further feedback. More details on behavioural results can be found in Kern et al. (2024).

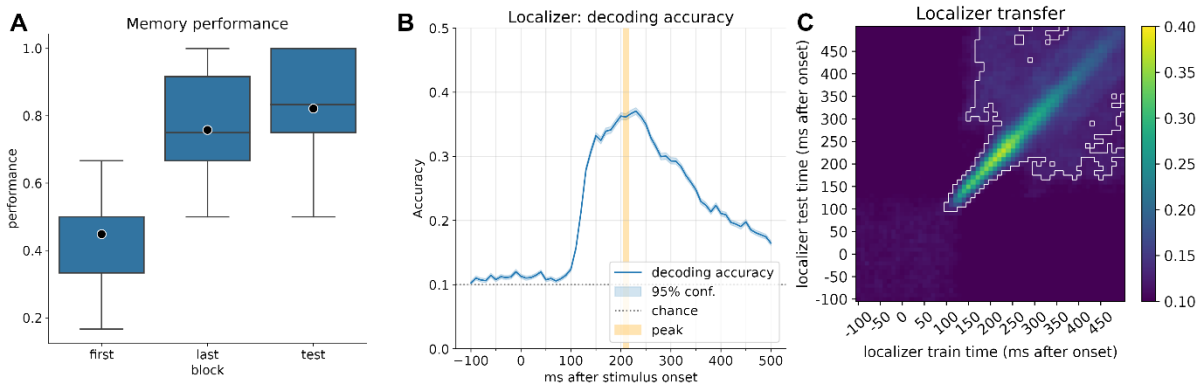

Figure 2 A) Memory performance of participants after completing the first block of learning, the last block of learning (block 2 to 6, depending on speed of learning), and retrieval performance after the resting state. B) Decoding accuracy of the currently displayed item during the localizer task for participants with a decoding accuracy above 30% (n=21, 4 participants' data did not pass this criterion). The mean peak time point across all participants corresponded to 210 ms, with an average decoding peak accuracy of 42% (n=21). Note that the displayed graph combines accuracies across participants, where peak values were computed on an individual level and then averaged. Therefore, at a group level the individual mean peak does not necessarily correspond to the average peak. C) Classifier transfer within the localizer when trained and tested at different time points as determined by cross validation, after ~200 ms, most training and testing time points generalize to each other (significant clusters indicated by cluster permutation testing, alpha<0.05).

Decoder training

As previously described in Kern et al. (2024), we trained classifiers on data from the localizer task, where participants were presented with images from the learning task in a pseudorandom order. These showed good decoding from brain activity, at a level comparable to previous reports as determined in cross-validation (~42% across all participants, range 32–57%, chance level: 10%, excluding participants with peak accuracy <30%). We used the averaged peak decoding accuracy

time point of 210 milliseconds across all participants (Figure 2B) to train final participant-specific decoders to apply on resting state data.

No sequential replay during resting state

In applying trained decoders to the resting state session, we used probability estimates of the ten classes as input to TLDM. In brief, TDLM quantifies time-lagged reactivation ("sequenceness") of states according to expected transitions, e.g. quantify how strongly state A->B was reactivated with a temporal distance of N milliseconds. We found no evidence for sequential replay measurable during the post-learning resting state. More specifically, the GLM did not exceed significance thresholds (conservative or liberal criterions) for any individual time lag, either in forward nor backward direction (Figure 3A). Additionally, we calculated the difference between the pre-resting state and post-resting state sequenceness values, to remove potential systemic biases on sequenceness fluctuation present in both sessions. We calculated an FDR corrected paired t-test for all 30 time lags individually, for forward and backward sequenceness between pre- and post-resting state respectively. All time lags were non-significant ($p_{FDR}>0.05$; without correction, three time points were significant: forward 100 ms, t=-2.43, p=0.024 and 240 ms, t=2.13, p=0.045, backward 200 ms time lag, t=-2.11, p=0.047). However, as noted in Y. Liu, Dolan, et al., (2021), correct statistical analysis of sequenceness scores is non-trivial and FDR-correction might be too conservative. Therefore, we also calculated a 1-sample-cluster-permutation-test of difference values with 10.000 permutations that considers the temporal correlation of time lag bins, and this revealed a single non-significant cluster at 230-240 ms forward (p=0.44). For a visualization of the reported differences see Figure 3B.

Additionally, we ascertained whether there was an interaction between memory retrieval performance and individual sequenceness strength by calculating the time lag of peak sequenceness across all participants (control forward = 100 ms, control backward: 10 milliseconds, post-learn forward: 280 ms, backward: 240 ms) and correlating the individual sequenceness values with the participants' performance. Neither was there a significant correlation between peak sequenceness scores and memory performance at post-learning resting state (forward r=0.0, p=0.99, backward: r=0.02, p=0.935, see Figure 3C), nor with the performance difference between post-rest retrieval minus the performance of the last block before rest (see Supplement Figure 10)

Lastly, similar to Liu et al. (2019), we split the 8-minute resting state into eight discrete time-bins and assessed replay strength for each segment separately (Figure 4). In none of these bins was a maximum permutation threshold exceeded. A more lenient 95% permutation threshold was exceeded in one segment of the post-learning resting state for time-bin 4 (20 ms backward

sequenceness). However, here the sequenceness value was negative suggesting, if anything, suppression of replay. Individual sequenceness curves for all segments can be found in Supplement Figure 5.

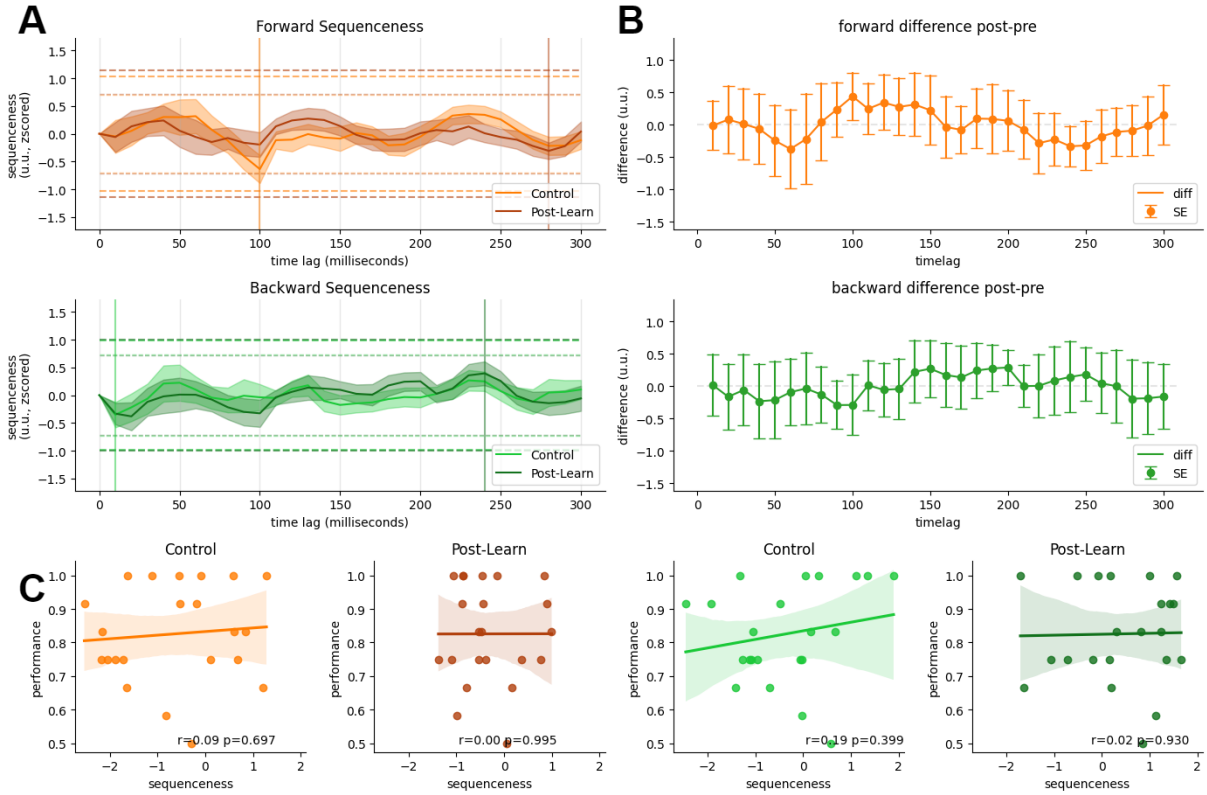

Figure 3 A) Forward and backward sequenceness values on the y-axis at different time lags (x-axis) for control resting state (light coloured) and post-learning resting state (dark coloured). Two significance thresholds are indicated, the more lenient 95% quantile of the maximum sequenceness of all permutations (lightly dotted line) and the maximum mean peak sequenceness across all permutations of all subjects (bold dotted line). None of the thresholds were surpassed. The peak mean sequenceness has been marked by a vertical line respectively. B) Difference between pre-learning and post-learning resting states across time lags. Using FDR-corrected paired t-tests for each time lag revealed no significant difference between conditions (without correction three sequenceness differences were significant: forward 100 ms, p=0.024 and 240 ms, p=0.045, backward 200 ms, p=0.047). An additionally performed cluster-permutation test found a non-significant cluster at 230-240 ms forward direction (p=0.44). Bands indicate two standard errors of the mean of the difference scores. C) Individual participant's retrieval memory performance relative to their sequenceness values at the peak mean sequenceness (indicated in A). Regression lines and 95% confidence intervals are fitted. For correlation with performance deltas between post and pre resting state retrievals see Supplement Figure 10. For individual sequenceness curves, see Supplement Figure 4.

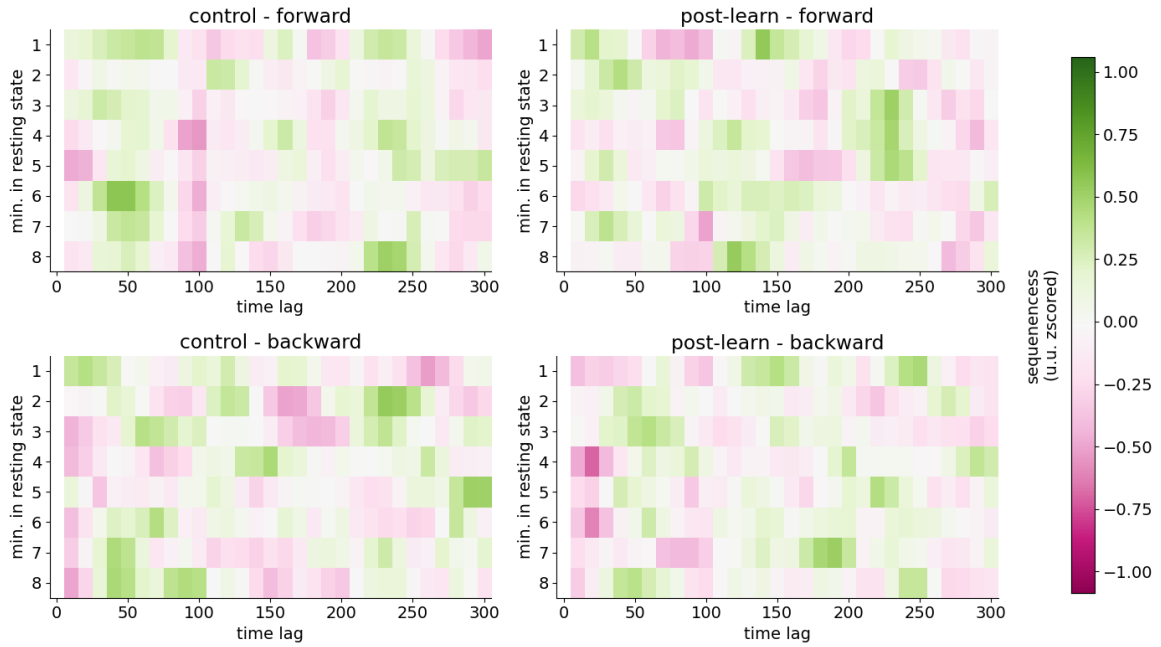

Figure 4 Sequenceness (heatmap) separately for each of the eight minutes of resting state on the y-axis, and different time lags on the x-axis. For each minute, we took either the first or second half of 30 seconds for the final calculation and the other 30-second segment for the exploration data set. Sequenceness crossed the 95% permutation threshold in the post-learning resting state in minute 4 (backward 20 millisecond time lag) alone. However, the sequenceness score was negative, rendering its interpretation non-trivial. Note that we did not apply any control for multiple comparisons across the segments.

Interim discussion

Overall, in the resting state recording directly after a learning block we could not reliably detect evidence for sequenceness using TDLM. This involved using previously implemented protocols in terms of localizer recording, pre-processing and decoder settings, albeit within a different cognitive protocol compared to those previously implemented within resting states (Y. Liu et al., 2019; Nour et al., 2021, 2023; Wimmer et al., 2020). Even though we found a single time lag with putative replay during one of the thirty-second segments, the evidence here was weak and thus its validity is questionable. Firstly, multiple comparison correction would have removed the effect. Second, interpretation of negative sequenceness values is unclear. As forward and backward sequenceness are estimated separately, in our interpretation, negative forward sequenceness suggests an expected sequenceness is replayed *less* than expected, which could be interpreted as replay suppression. One possible way this could occur is via a repetition suppression process (Schwartenbeck et al., 2023), if one assumes that activation of one item occurs simultaneously with the next in line and

subsequently that pattern of neuronal activity is suppressed. However, this appears to us, at best, a convoluted argument. Additionally, recent reports suggest replay avoids self-repetition in addition to avoidant of replay for just experienced episodes (Mallory et al., 2025),which would show as negative sequenceness. However, this effect has so far been shown to occur on a time-scale of seconds and not minutes.

Previous reports using TDLM during resting state involved paradigms with a dominant inference component (Y. Liu et al., 2019; Y. Liu, Mattar, et al., 2021; Nour et al., 2021)**.** In our study, we used a declarative graph-based paradigm that lacked this inferential component. We note previous research in humans has shown reactivation and replay during rest in the context of non-inferential paradigms using fMRI (Ogawa et al., 2024; Schapiro et al., 2018; Tambini & Davachi, 2013), and especially in the context of declarative learning (using fMRI&EEG: Deuker et al., 2013; using intracortical electrodes: Eichenlaub et al., 2020; using fMRI: Schlichting & Preston, 2014; using intracranial EEG: Zhang et al., 2018). On the other hand it has been reported that replay is more likely to be expressed for weakly encoded memories (Denis et al., 2020; Schapiro et al., 2018) and hence might be absent if encoding strength is too strong. While we employed criterion learning at 80% for this reason, as is usual in sleep and memory research, we cannot be certain if this represents a level of encoding strength that obviated task-related replay in our study. Some anecdotal evidence for replay occurrence might come from many participants reporting involuntarily seeing segments of the sequence flashing in front of their eyes during the resting state, though we caution that there is mixed evidence for a link between anecdotal reports of conscious experience as an indicator for replay (Komsky, 2015; Wittkuhn et al., 2024).

As we did not know whether lack of evidence for replay was inherent to our paradigm, in a second study, we explored potential explanations for this null finding by conducting a hybrid simulation study that combined localizer data and data from a control resting state. This simulation allows quantification of the strength of replay necessary in our paradigm for it to be detectable using the TDLM methodology.

Results Study II: Simulation

In this hybrid simulation study, we enriched the control resting state data of participants with simulated replay events. I.e., we inserted sequences of neural patterns extracted from the localizer (taken from the time point of peak decoding accuracy) into the control resting state with a state-to-state lag of 80 milliseconds. We varied the density of replay, traditionally denoted as “replay events per minute” (min^{-1}) and looked at resulting sequenceness strengths. Additionally, we scaled the replay density inversely with the participant’s retrieval memory performance to simulate a putative

increase of replay for less stable memories (e.g. a participant with lowest, i.e. 50% memory performance would have a factor 1.0 applied to their replay amount, while a participant with highest, i.e. 100% memory performance would show reduced replay and have a scaling factor of 0.5 applied to the number of inserted replays). We used different scaling factors to explore how they contribute to relationships between measures of sequenceness and memory performance. While we acknowledge the relation between replay and memory performance is probably more complex (Kern et al., 2024; Schapiro et al., 2018; Wimmer et al., 2020), we applied this simplified scaling to assess whether TDLM can detect behavioural correlations with sequenceness strength, as has shown previously (Kern et al., 2024; Y. Liu et al., 2019; Nour et al., 2021; Wimmer et al., 2020; Yu et al., 2023). Our results indicate that replay and correlations with behaviour were only detectable at very high - putatively biologically implausible - densities.

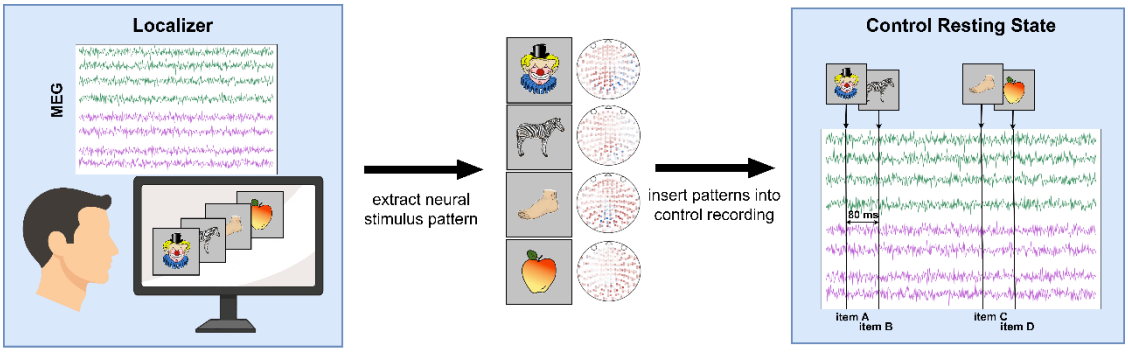

Figure 5. Schematic of procedure for inserting simulated replay into the control resting state. First, neural patterns are extracted, for each stimulus, from the peak of decodability during the localizer task. Participant-specific patterns are normalized by subtracting the average sensor values of seeing any stimulus from the sensor values of seeing only the stimulus of interest. Next, these subtle patterns are inserted into the control resting state at a fixed interval, following a one-step transition pattern according to the task sequence. A refractory period is retained between each replay event to prevent overlaps. For details see Methods section.

Sequenceness only detectable at very high replay density

Our simulation analysis found that a replay density of 150 min^{-1} and a density of 80 min^{-1} were necessary in order to reach the maximum and 95% quantile permutation threshold, respectively (see Figure 6A). Figure 6B shows sequenceness curves for selected densities at 0 min^{-1} (baseline), 40 min^{-1}, 80min^{-1} and 120min^{-1}. At 40 min^{-1} only a small increase of sequenceness above baseline is detectable. Note a significant drop of sequenceness at 100 milliseconds, due to the alpha control introduced at 10 Hz by inserting repeating patterns of the decoded items (Y. Liu, Dolan, et al., 2021). The alpha correction likely over-corrected and introduced negative sequenceness at 10 Hz seen in some participants. Therefore, we included the analysis without the alpha-correction in the Supplement Figure 6. NB the strong negative sequenceness at 100 millisecond time lag was not present in our exploratory data set and only appeared in the data that was held back for the final calculation (as

preregistered, we used 50% of the resting state data for exploration and parameter search and report here on the unseen 50% after parameters were chosen, see Methods section for details).

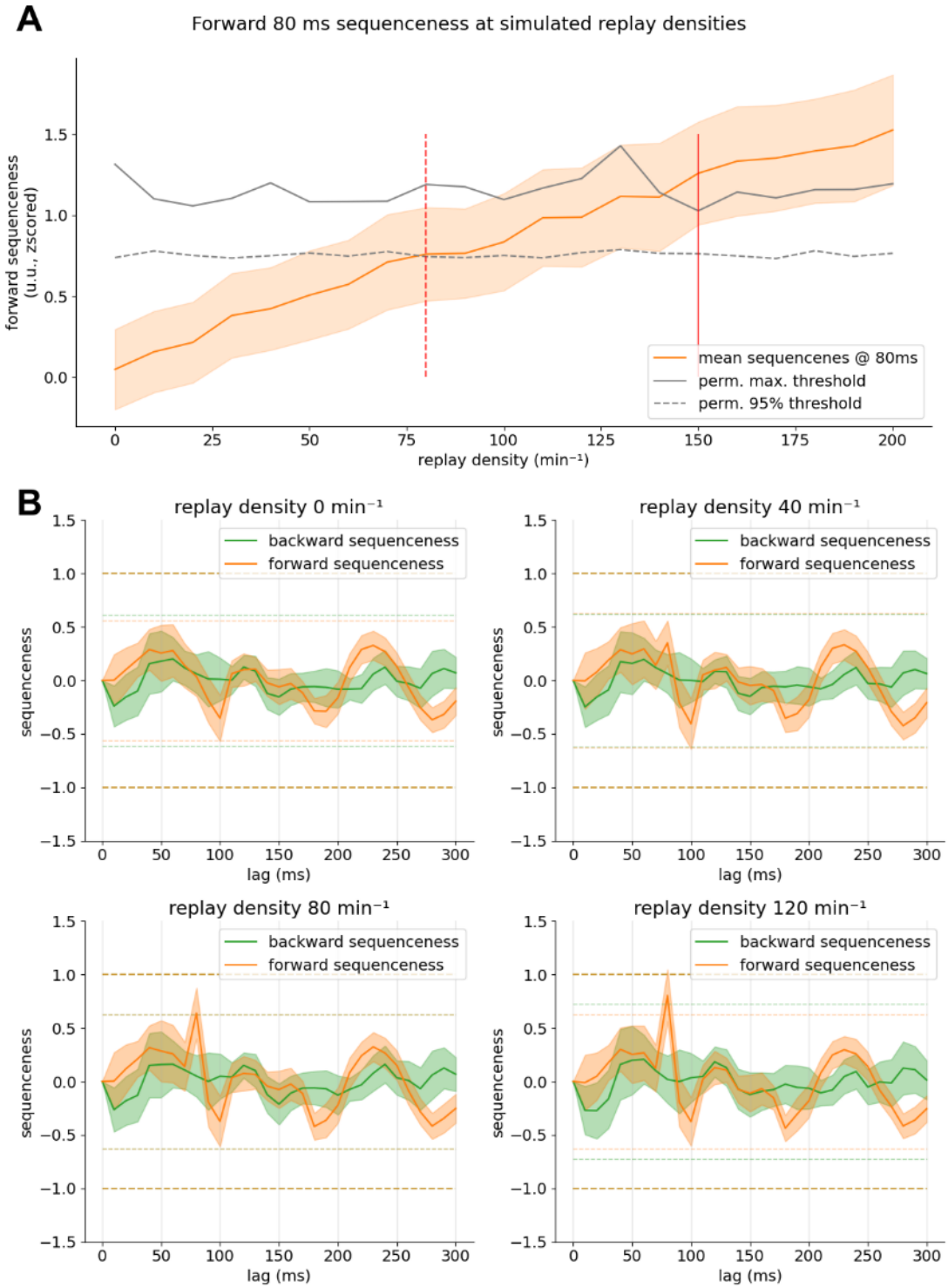

Figure 6. A) On the y-axis, sequenceness at 80-millisecond state-to-state time lag, at different replay densities on the x-axis with standard error as shaded orange. The 95% confidence interval significance threshold is reached at a density of ~80 min^{-1}, while the maximum permutation threshold is reached only around 150 min^{-1}. B) Sequenceness across time lags for replay at baseline (0 min^{-1}) and simulated for a density of 40, 80 and 120 min^{-1} with a simulated time lag of 80 milliseconds.

274

275 **Correlation with behaviour only present at high replay speeds**

The correlation of behaviour with sequenceness at 80 milliseconds time lag was non-significant, even at high replay densities of 200 min^{-1} (see Figure 7A). Here we assumed a realistic scenario that linearly downscales replay density with increasing performance from 100% to down to 50% for increased memory performance. To amplify the correlation effect, in a secondary analysis, we normalized the performance scaling between 100-0% (i.e. 100% performance would lead to 0% of replay inserted). In this maximum-scaling scenario, the correlation of sequenceness with performance was markedly boosted, yet only reached significance at a density of 200 events min^{-1}. When further investigating this lack of strong influence of our scaling, we found that even in the baseline condition without simulated replay (0 min^{-1}), the correlation with performance seems to oscillate, depending on which time lag it is computed on (Figure 7B), indicating fluctuations of sequenceness between participants that are non-random. If we chose a different time lag for our simulation, added effects of baseline plus simulation would have probably reached significance more easily (e.g. 210-millisecond time lag). This baseline variation becomes apparent when comparing sequenceness of participants at baseline with sequenceness values boosted via simulated replay at 80 millisecond time lag: Even in the baseline condition (0 events min^{-1}, Figure 7D), some participants express higher sequenceness values than other participants with simulated replay of 160 min^{-1}. This indicates that the effect that we wanted to introduce via scaling the inserted events with memory performance is overshadowed by some form of bias present at baseline, that induces marked variations in sequenceness without any replay present, even after a recommended GLM-based alpha control (Y. Liu, Dolan, et al., 2021).

The resulting correlation is of moderate size even at higher densities (Pearson's r of around -0.2-0.3), indicating that our paradigm was likely underpowered for this specific analysis. Therefore, we performed a bootstrapped power analysis by oversampling existing participants, with 10,000 repetitions per sample size. We found that more than 90 participants would have been necessary to detect a correlation between performance and sequenceness in the simulated density of 80 min^{-1} condition (Figure 7C) with 80% power with the above-mentioned maximum scaling applied. Nevertheless, one should keep in mind that this increase in power might also lead to increase power to detect effects introduced by nuisance effects in the baseline condition.

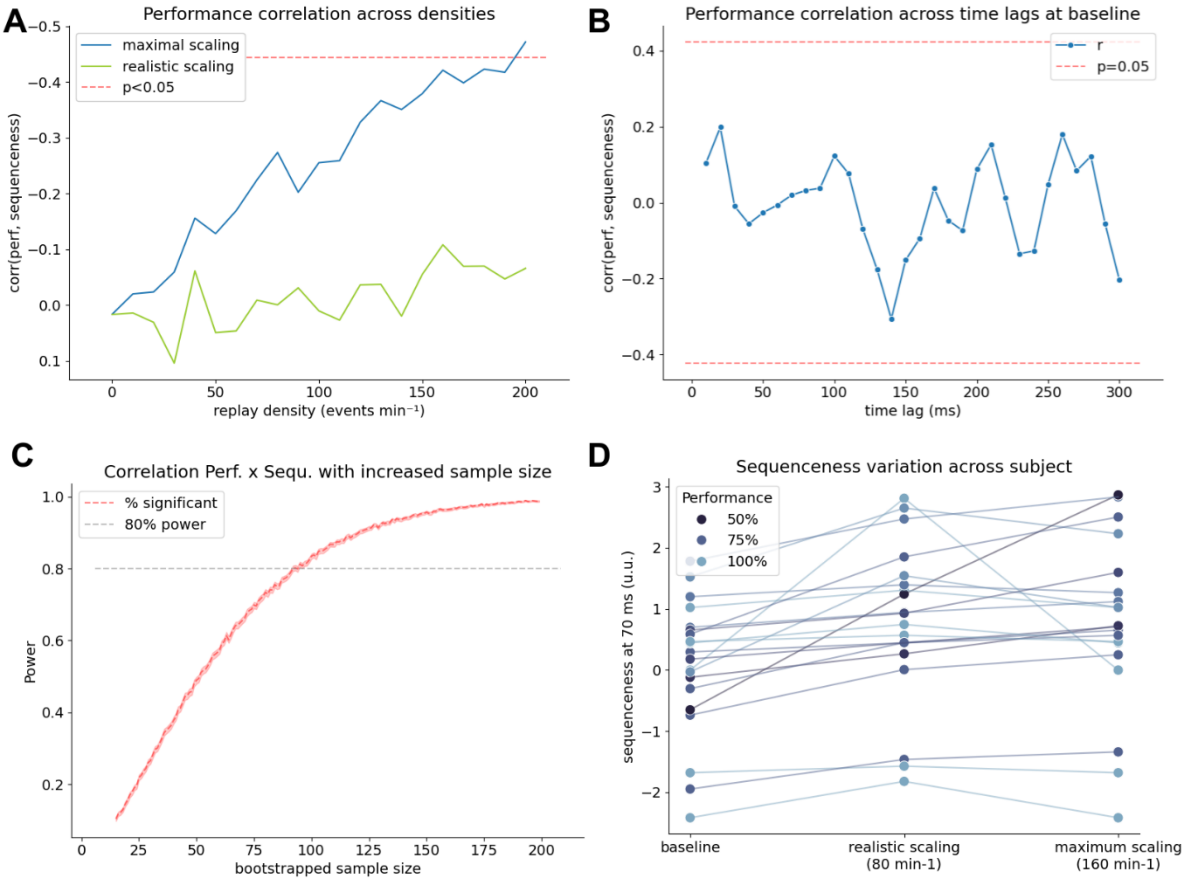

Figure 7 A) *Relationship (Pearson's r) between memory performance (behaviour) and sequenceness at 80 ms time lag on the y axis, with replay density on the x-axis for two scaling rules: Realistic scaling: Replay density was inversely scaled with participant's performance by 50-100% (i.e., the worst performer had 100% while the best performer only had 50% of replay density). Maximal scaling: Replay density was scaled in from 0-100% (i.e., the best performer had no replay inserted). Significance of the correlation is only reached in the maximum scaling case at around 200 min^{-1}. B) Correlation of sequenceness computed across different time lags in the control condition (i.e., without inserted replay). Even when no replay is present, the correlation fluctuates significantly depending at which time lag it has been computed, possibly due to baseline variations that fluctuate differentially between participants. C) Bootstrap power analysis showing how many participants would be necessary to detect a significant correlation between replay and performance in the maximally scaled scenario with a replay density of 80 min^{-1}. 80% power to detect a correlation is reached around a sample size of around 90. D) Sequenceness at 80 milliseconds time lag in the control condition (left), in the realistic scenario with replay scaling from 50-100% (middle) and the maximal scenario with scaling from 0-100% (right). Participant's performance is indicated by increasing saturation of blue. While all participants show an increase in sequenceness with increased scaling, some participants have a higher sequenceness value and an ordering according to performance is barely visible in the maximum scaling case.*

Discussion

Using temporally delayed linear modelling (TDLM), we investigated whether sequential replay of learned graph-structured associations could be detected during a post-learning resting state. Contrary to an expectation based on previous findings, we did not find evidence for replay of well-learned sequences. This was despite using a similar methodology to that used in prior replay investigations of resting state following an associative learning task, albeit these involved different paradigms (Eldar et al., 2020; Q. Huang et al., 2024; Y. Liu et al., 2019; Nour et al., 2021; Yu et al., 2023). However, due to differences from previously used paradigms, we cannot conclude that lack of evidence for replay reflects on the sensitivity of our detection method (TDLM) or reflects that our task was not eliciting sufficiently strong resting state replay to enable replay detection using TDLM.

Based on the above, we designed a simulation study to exploring the strength of replay that would be necessary for successful detection. This simulation study represented an effort to explain our null findings in relation to the potential sensitivity of TDLM. By inserting synthetic replay events into pre-task resting state data we show that replay would only be detectable under an assumption of very high replay rates— with more than 80 replay events per minute necessary to reach significance thresholds. Here, one “replay event” is defined as a train of sequential reactivations with a certain state-to-state time lag, i.e., 80 ms, meaning more than one replay event per second on average throughout the entire resting state. Furthermore, we find that already at baseline (i.e. without any replay) sequenceness values are biased by yet unknown confounders that introduce absolute offsets in baseline sequenceness values between participants.

Our simulation indicates that when an increase in sequenceness by actual replay is introduced, the baseline offset between participants is larger than the increase at the group level. Therefore, correlating behavioural measures with individual sequenceness values should be regarded with caution unless this baseline offset is controlled for. Our findings highlight a potential need for further methodological refinements in both experimental paradigms and analysis techniques to reliably detect human replay during extended offline periods (such as resting state or sleep) using non-invasive measures. Finally, we provide recommendations for future studies and suggest ways to enhance the reliability of replay detection methods.

High replay density necessary to detect sequenceness

In our study, more than one replay event per second (80 min^{-1}) would have been necessary to detect replay at a group level. Sharp-wave-ripples (SWR) are traditionally considered as substrates for memory reactivation and hence strong replay expression (Eschenko et al., 2008b; Joo & Frank, 2018; Roumis & Frank, 2015), with each SWR containing several sequential item reactivations. While every SWR might not contain task-relevant activity (Schreiner et al., 2024), their occurrence rate is a

reasonable proxy to estimate *in vivo* replay density. Previous research in rodents has reported that ripple rate significantly varies between tasks and states, being most prominent in offline states such as NREM and post-task rest at a replay density of around 20-25 events per min^{-1} (Eschenko et al., 2008b; Ponomarenko et al., 2003; Wiegand et al., 2016). In humans, evidence from intracranial recordings is sparse, but studies estimate a ripple density of between 1-15 min^{-1} during NREM sleep (X. Jiang et al., 2020; Ngo et al., 2020) and ~1.5-4 min^{-1} during resting state (Y. Y. Chen et al., 2021). However, it should be noted that reported ripple rates depend on an applied detection criteria and so might underestimate their actual occurrence (A. A. Liu et al., 2022). While *in vitro* studies have reported that CA1/CA3 neurons can maintain a (experimentally induced) density of up 50-200 min^{-1} (Buzsáki, 2015; H. Jiang et al., 2018; Kanak et al., 2013), to our knowledge, such densities have not been reported *in vivo*.

As replay was detectable at around 80 min^{-1} (~1.33 replay events per second), with more strict thresholds only being reached at around 150 min^{-1} (~2.5 replay events per second). Based on previous research it might be considered implausible that these densities would be maintained by the brain throughout an 8-minute resting state. Nevertheless, as it is known that SWRs occur in bursts (Buzsáki, 2015), and it is conceivable that higher ripple rates are maintained during shorter time windows, as for example during short intervals of recall, where they can reach more than 40 min^{-1} (Norman et al., 2019).

Interestingly, Higgins et al. (2021) report that replay events detected by TDLM were not evenly distributed throughout the resting state and, even though not explicitly reported, varied between 9-40 min^{-1} for different segments of an exemplar participant. When replay occurs in bursts, certain time windows might reach necessary density thresholds, while averaging over larger windows might be inconclusive. However, such windows would need to be selected on some principled basis to avoid inflating false positive rates. Nevertheless, in our post-hoc analogue sub-analysis of 30-second individual segments of the resting state, no clear evidence for replay was detectable. Currently, in the context of MEG replay studies it is not reported what replay rates (events min^{-1}) are assumed. Therefore, future studies might consider providing estimates for replay rates under which reported findings are plausible, analogous to SWR rates reported in animal studies, e.g. via simulations.

Correlation with behaviour is overshadowed by baseline fluctuation of sequenceness

The occurrence of replay, in the absence of ground truth, can to some extent be validated by a correlation between a replay measure and behavioural performance (Y. Liu, Mattar, et al., 2021; Wimmer et al., 2020). In our simulation, we were not able to induce a strong relationship of sequenceness to participants' performance at realistic replay densities. Even in an unrealistic,

maximal-scaling scenario, with no replay for the best-performing and 100% replay for the worst-performing participant, correlations were only significant at implausibly high replay densities of around 200 min^{-1}. A power analysis revealed that around 90 participants would have been necessary to establish a correlation in the maximum scaling case at a density of 80 min^{-1}. We find that the magnitude of baseline sequenceness values across participants was higher than the induced effects and was hence not affected strongly by inserting synthetic replay (see Figure 7D).

Spurious sequenceness in the control condition

In data without any expected replay sequenceness should be close to zero or else be attributed to noise or bias. While random noise should average out with increasingly large number of participants, it remains possible that a systemic bias is shared among participants. For example, this might be the case with alpha oscillations. In our study, non-significant fluctuations in sequenceness already occurred in the control condition, a phenomenon not unique to this study (and reported in supplementary material of Nour et al., 2021, 2023 and Liu et al., 2019). Thus, it seems as if a yet unknown bias introduces spurious systematic sequenceness effects that, in our simulation, may serve to overshadow actual sequenceness at low densities. While, as previously discussed (Liu, Dolan, et al., 2021; Liu et al., 2019), endogenous oscillations such as eyes-closed-alpha can affect TDLM, the spurious (albeit non-significant) sequenceness in our case was not sufficiently controlled by alpha correction to make it disappear completely (see Supplement Figure 6 for analyses without the 10 Hz correction method). Interestingly, the sign of the correlation discussed above fluctuates approximately at a 10 Hz rhythm, leading us to speculate that alpha oscillations may affect baseline sequenceness in a manner not removed by controlling for alpha using recommended methods (Liu, Dolan, et al., 2021). Furthermore, we speculate that other factors might be contributing to spurious sequence detection, for example oscillatory inter-trial-coherence during localizer training (Hoffman et al., 2013; Kragel et al., 2020; van Diepen & Mazaheri, 2018), (phase)-coupling of two or more oscillations (Fell & Axmacher, 2011; Watrous et al., 2015) or phase-differences in travelling waves (Hughes, 1995; Muller et al., 2018). Exploring these possibilities is beyond the scope of the current study and should be evaluated systematically in future experiments.

Finally yet importantly, it is important to consider that endogenous oscillations might play a functional role. Thus, it has been proposed that certain theta phases support encoding -and consolidation (Hasselmo et al., 2002; Kerrén et al., 2018, 2022), or that oscillations provide a window for reactivation (Higgins et al., 2021; Staresina et al., 2015). Such a scenario poses a challenge for differentiating between a theta-phase-bias, not attributable to memory processing, from actual reactivation present only during a specific phase of an oscillation.

Probing the conditions under which TDLM works requires realistic simulations

Previous studies performed sequenceness analyses on simulated replay, but replay density has rarely been simulated under realistic conditions. For example, in the sample code of Liu, Dolan, et al., (2021), replay was simulated with a density of 2000 min^{-1}. Similarly, in Liu, Mattar, et al., (2021), a density of 2400 min^{-1} was used. Re-running these simulation scripts, with arguably a more realistic replay density (i.e. 15min^{-1} for NREM, as found in X. Jiang et al., 2020) , sequenceness failed to reach significance, even with purely synthetic data (Supplement Figure 7B). Additionally, purely synthetic data probably over-estimates sensitivity, as it lacks the previously discussed systemic bias that can introduce spurious sequenceness into control resting states. Using control dataset as a simulation basis, as implemented here, mitigates this bias and we suggest it provides a better approximation of real effects. Similarly, using entirely synthetic data may overestimate decodability of reactivations when transferring decoders from a localizer to another modality, as patterns are probably less well separable within a testing condition compared to a training condition (cf Supplement Figure 7E and Supplement Figure 2).

TDLM at its core is a parameter-free method. Nevertheless, a large space of decoding modalities exist that can influence an analysis outcome. In this paper we primarily applied default choices as previously reported (L1 Logistic Regression trained on peak decoding time point as in Kern et al., 2024; Kurth-Nelson et al., 2016; Y. Liu et al., 2019; Nour et al., 2021; Wimmer et al., 2020, 2023). Nevertheless, we note many different parameter combinations have been applied in other studies and their combined effect remains unclear (Eldar et al., 2020; Q. Huang & Luo, 2023; Wimmer et al., 2020; Wise et al., 2021). For example, here we observed that mean baseline probabilities produced by the classifier vary per participant (Supplement Figure 2). While probabilities increased more or less linearly across all participants, we opted to normalize these by dividing the mean probability per class per participant. Similarly, in an exploration dataset, we observed that sequenceness effects were driven by a few participants who produced high magnitudes of sequenceness scores. To mitigate these effects, we z-scored sequenceness for each trial, as reported previously (Wimmer et al., 2020; Yu et al., 2023). However, this approach also has its drawbacks, as it could potentially deflate true events in participants with good decodability and so inflate false positives, and vice versa. Furthermore, many different classifier regimes have been used in the context of TDLM (e.g. Lasso Logistic Regression vs SVM, sensor-based decoding vs. temporal embedding with PCA, normalization of sequenceness scores via z-scoring vs no normalization, using classifier raw decision values vs probability estimates, binary-class training vs multi-class training to only name a few). It remains unclear how these, and especially their combinations, impact TDLM's

ability to differentiate true sequenceness results from a systemic bias due to, for example, to endogenous oscillatory confounders. To improve methodological certainty, further studies could usefully investigate this question in form of a multiverse re-analysis of previously published data (Chambers, 2020; Dafflon et al., 2022).

Improving TDLMs sensitivity

TDLM is a complex and sophisticated approach for detecting human replay. However, in our study, TDLM was not sufficiently sensitive to detect replay during offline periods, under an assumption that replay was indeed present in this 8-minute rest-period. Nonetheless, we suggest several factors could potentially be improved to increase its power and sensitivity. First, the success of the approach hinges on the quality of the decoders. Improving their specificity as well as their ability to transfer from the localizer to a condition of interest should be assessed more closely. While most decoding approaches simply assume that transfer is seamless, previous research has indicated that this depends heavily on target modality, such as the way the decoders are trained as well as the cognitive processes involved (Bezsudnova et al., 2024; Dijkstra et al., 2019, 2021). Further research should optimize, and validate, that decoders trained primarily on sensory evoked activity can be flexibly be applied to replay detection, for example by introducing a control that demonstrates classification accuracy in relation to another sensory modality. If transfer is not possible from visual sensory to, for example auditory or imagined stimuli, it might indicate failure of representational transfer that is necessary for detection of reactivation during replay. Relatedly, focusing on the peak of the decodability probably introduces a reliance on sensory processing that does not necessarily transfer well to other, sensory and non-sensory, conditions. Thus, training decoders independently, or as an ensemble of the time dimension as, for example, as performed by Eldar et al. (2020) or Wise et al., (2021) could help circumvent this problem. Similarly, performing localizers on categorical stimuli instead of specific stimuli, as well as training on multi-sensory localizers, might prove fruitful.

Second, as our simulation shows, detecting replay in shorter windows of time should be possible, as here high replay density needed has previously been reported (Norman et al., 2019). Therefore, restricting the analysis to time ‘regions of interest’ wherein a high replay frequency is expected could drastically improve detection power. As it is known that replay occurs in bursts, such windows might exceed necessary replay densities. While studies researching planning or retrieval naturally offer such restricted analysis windows, this becomes more difficult for longer recordings such as resting state and sleep analysis. Furthermore, to prevent false positives and “double-dipping” (Kriegeskorte et al., 2009), such time-windows would need to be chosen beforehand or include an appropriate control for multiple-comparisons. Furthermore, detection might be enhanced through use of contrasts of specified oscillation phases (e.g. slow oscillations during sleep or theta phases

during resting state) during which it is known that replay typically occurs (Xiao et al., 2024). Another approach would be contrasting windows after targeted memory reactivation cues and respective control phases of control stimulation to validate the replay detection (Z. Chen et al., 2024). Last but not least, search windows could also be artificially narrowed by using a sliding window similar to the approach implemented by Wise et al., (2021), however, in this case multiple comparison problems between different windows are introduced and circular testing would need to be avoided (e.g., by using exploration and validation datasets).

Limitations

In an effort to explain null-findings, we conducted a simulation study. Despite close attention to the bounds of this simulation, it is possible that the reported results are unique to our analysis pipeline or recording device (e.g. application of MaxFilter, see Methods section), even though we rigorously followed best practices of the field. While we are reasonably confident the proposed approach approximates expected veridical replay situations, certain assumptions of our analysis may be too strong and not model actual replay well (e.g. the way we chose to extract and insert neural patterns). Furthermore, it is possible that TDLM behaves differently with different MEG systems, different paradigms, pre-processing or different analysis approaches and that we simply did not find the correct parameters to make it work. Nevertheless, we closely followed previous pipelines applied on the same dataset (Kern et al., 2024) that did find effects using TDLM and also tried many plausible alternative pipelines without success. Additionally, while the analysis we propose arguably simulates replay under more realistic conditions than previous work, there are still ways to increase realism even further, that were out-of-scope for this paper. Future studies could for example simulate nesting of replay with oscillations such as gamma or theta or look how clustered replay affects sequenceness.

Conclusion

We were unable to detect replay during an eight-minute rest epoch in our data set using TDLM. Conducting a simulation, we first show that even if replay was present, implausibly high replay densities would be necessary to achieve significance at our sample size. Second, despite our best efforts, we were unable to induce a correlation of sequenceness with behaviour at the individual level, and uncovered large baseline fluctuations in sequenceness across participants. Taken together, our results suggest that future studies should refine and validate decoder training paradigms and limit the search space for successful replay detection during resting states via TDLM. Additionally, future studies should calculated expected replay densities that would be necessary for reported results to demonstrate plausibility. Finally, our results highlight the overall importance of delineating the limits of replay detection for the interpretation of null effects.

Methods Study I: Resting State Analysis

Participants

Note that parts of this methods section are taken from Kern et al. (2024) for convenience of the reader. We recruited thirty participants (15 men and 15 women), between 19 and 32 years old (mean age 24.7 years). Inclusion criteria were right-handedness, no claustrophobic tendencies, no current or previous diagnosed mental disorder, non-smoker, fluency in German or English, age between 18 and 35 and normal or corrected-to-normal vision. Caffeine intake was requested to be restricted for four hours before the experiment. Participants were recruited through the institute's website and mailing list and various local Facebook groups. A single participant was excluded due to a corrupted data file and replaced with another participant. We acquired written informed consent from all participants, including consent to share anonymized raw and processed data in an open access online repository. The study protocol was approved by the ethics committee of the Medical Faculty Mannheim of Heidelberg University (ID: 2020-609). The experiment and analysis were preregistered at aspredicted.org (https://aspredicted.org/kx9xh.pdf, #68915).

Procedure

For brevity, we only summarize the task design and procedure here. All details on the localizer, learning and retrieval task as well as the stimulus material can also be found in Kern et al., (2024). Participants came to the laboratory for a single study session of approximately 2.5 hours. After filling out a questionnaire about their general health, their subjective sleepiness (Stanford Sleepiness Scale, Hoddes et al., 1973) and mood (PANAS, Watson et al., 1988), participants performed five separate tasks while in the MEG scanner. First, before any stimulus exposure, an eight-minute eyes-closed resting state was recorded. This was followed by a localizer task (~30 minutes), in which all 10 items were presented 54 times in pseudo-randomized order, using auditory and visual stimuli. Next, participants learned a sequence of the 10 visual items embedded into a graph structure until they achieved 80% accuracy or reached a maximum of six blocks (7 to 20 minutes). Following this, we recorded another eight-minute eyes-closed resting state to allow for initial consolidation and, finally, a cued retrieval session (four minutes), of which the results have previously been reported in Kern et al., (2024). For an overview, see Figure 1. For an animated version of the task, see GitHub pages at https://cimh-clinical-psychology.github.io/DeSMRRest-TDLM-Simulation/.

Localizer task

Ten stimuli were shown to participants repeatedly in a pseudo-randomized order with 54 presentations per image. They were drawn images from Rossion & Pourtois, (2001), selected to be diverse in colour, shape and category. In each trial, a fixation cross was shown and after 0.75-1.25 seconds a word describing the current stimulus was played via headphones. Next, the stimulus image was shown for 1 second. As a distractor, in ~ 11% of the trials the audio and image were incongruent, which participants should indicate with a button press.

Graph Learning

The ten images were randomly assigned to nodes of the graph, as shown in Supplement Figure 1. Participants were instructed to learn a randomized sequence of elements with the goal of reaching 80% performance within six blocks of learning. During each block, participants were presented with each of the twelve edges of the graph exactly once.

After a fixation cross of 3.0 seconds, a first image was shown on the left of the screen. After 1.5 seconds, the second image appeared in the middle of the screen. After another 1.5 seconds, three possible choices were displayed in vertical order to the right of the two other images. One of the three choice options was the correct successor of the cued edge. Of the two distractor stimuli, one was chosen from a distal location on the graph (five to eight positions away from the current item), and one was chosen from a close location (two to four positions away from the current item). Feedback was shown for 3 seconds. No audio was played during learning. After completing the task, participants were told that their knowledge would be prompted once more a few minutes later (see retrieval).

Resting State

Two resting state recordings were recorded in the MEG. One before any stimulus exposure at the beginning of the experiment (pre-RS), as well as a second one (post-RS) graph learning, before the retrieval part. Each resting state session lasted eight minutes. Participants were instructed to close their eyes and to “not think of anything particular”.

Retrieval

After the resting state, we presented participants with a single retrieval session block, which followed the exact layout of the learning task with the exception that no feedback was provided as to whether entered choices were correct or incorrect (Supplement Figure 1D).

MEG Acquisition and Pre-Processing

MEG was recorded in a passively shielded room with a MEGIN TRIUX (MEGIN Oy, Helsinki, Finland) with 306 sensors (204 planar gradiometers and 102 magnetometers) at 1000 Hz with a 0.1–330 Hz band-pass acquisition filter at the ZIPP facility of the Central Institute for Mental Health in Mannheim, Germany. Before each recording, empty room measurements ensured no ill-functioning sensors were present. Head movement was recorded using five head positioning coils. Bipolar vertical and horizontal electrooculography (EOG) as well as electrocardiography (ECG) was recorded. After recording, the MEGIN proprietary MaxFilter algorithm (version 2.2.14) was run using temporally extended signal space separation (tSSS) and movement correction with the MaxFilter default parameters (Taulu & Simola, 2006, raw data buffer length of 10 s, and a subspace correlation limit of .98. Bad channels were automatically detected at a detection limit of 7; none had to be excluded. The head movement correction algorithm used 200 ms windows and steps of 10 ms. The HPI coil fit accept limits were set at an error of 5 mm and a g-value of .98). Using the head movement correction algorithm, the signals were virtually re-positioned to the mean head position during the initial localizer task to ensure compatibility of sensor-level analysis across the recording blocks. The systematic trigger delay of our presentation system was measured and visual stimuli appeared consistently 19 milliseconds after their trigger value was written to the stimulus channel, however, to keep consistency with previous studies that do not report trigger delay, timings in this publication are reported uncorrected (i.e., ‘as is’, not corrected for this delay).

Trial data were pre-processed using Python-MNE (version 1.7, Gramfort, 2013). Data were down-sampled to 100 Hz using the MNE function ‘resample’ (with default settings, which applies an anti-aliasing filter before resampling with a brick-wall filter at the Nyquist frequency in the frequency domain) and ICA applied using the ‘picard’ algorithm (Ablin et al., 2018) on a 1 Hz high-pass filtered copy of the signal using 50 components. As recommended, ICA was set to ignore segments that were marked as bad by Autoreject (Jas et al., 2017) on two-second segments. Components belonging to EOG or ECG and muscle artifacts were identified and removed automatically using MNE functions ‘find_bads_eog’, ‘find_bads_ecg’ and ‘find_bads_emg’, using the EOG and ECG as reference signals. Finally, to reduce noise and drift, data were filtered with a high-pass filter of 0.5 Hz using the MNE filter default settings (hamming window FIR filter, -6 dB cutoff at 0.25 Hz, 53 dB stop-band attenuation, filter length 6.6 seconds). To improve numerical stability, signals were re-scaled to similar ranges by multiplying values from gradiometers by 1e10 and from magnetometers by 2e11. These values were chosen empirically by matching histograms for both channel types. As outlier values can have significant influence on the computations, after re-scaling, values that were still above 1 or below -1 were “cut off” and transformed to smaller values by multiplying with 1e-2.

Trials from the localizer task were created from -0.1 to 0.5 seconds relative to visual stimulus onset to train decoders. We realized that the initial pre-registered window of 0 to 0.3 seconds was rather short and we deviated from the pre-registration by extending the analysis window by 100 milliseconds before and 200 milliseconds after stimulus onset. However, the deviation was only to improve interpretability and to include baseline data and did not alter the results in any way. No baseline correction was applied. To detect artifacts, Autoreject was applied using default settings, which repaired segments by interpolation in case artifacts were present in only a limited number of channels and rejected trials otherwise. Anonymized and maxfiltered raw data are openly available at Zenodo, the localizer data has been previously published as part of a previous publication (v1 https://doi.org/10.5281/zenodo.8001755), the resting state data can be found at v2 (https://doi.org/10.5281/zenodo.15629081), code and behavioural data will be made public on GitHub at https://github.com/CIMH-Clinical-Psychology/DeSMRRest-TDLM-Simulation.

From the resting state, segments were taken between the onset and offset markers, which were approximately 8 minutes apart and in which the participant had the eyes closed. `Autoreject` is not well tested on longer segment data, therefore, unlike for the localizer trials, we did not apply it to the resting state data. However, a supplementary analysis revealed that both ICA and Autoreject did not have any significant effect on decoding accuracy, a result also reported in other studies (Delorme, 2022).

Split in exploration and validation dataset

As stated in the pre-registration, we used 50% of the resting state data for exploration to tune classifiers and try out different approaches. To mitigate time effects on replay, we used interleaved 30 second-segments of the resting state data to divide into exploration and validation sets. To counterbalance ordering effects, for the first 15 participants we concatenated the uneven segments as exploration, while for the latter participants switched the assignment. After settling for the parameters reported in this section, we used the other 50% of data to validate the results. All results described in study 1 are from the validation segments.

Decoding framework and training

We closely followed the approaches applied in previous research (Kurth-Nelson et al., 2016; Y. Liu et al., 2019; Wimmer et al., 2020) and using the same data set as reported in our previous study (Kern et al., 2024). We used Lasso regularized logistic regression on sensor-level data of localizer trials using the Python package Scikit-Learn (Pedregosa et al., 2011). Decoders were trained separately for each participant, and each stimulus, using liblinear as a solver with 1000 maximum iterations and a L1 regularization of C=9.1, which was determined by cross-validating the decoding accuracy in the

time span of 150-250 ms after stimulus onset across participants using values for C of a log-spaced interval from 10^{-2} to 10^{2} (see Supplement Figure *8* for details). To circumvent class imbalance due to trials removed by Autoreject, localizer trials were stratified such that they contained an equal number of trials from each stimulus presentation by randomly removing trials from over-represented classes. Using a cross-validation schema (leaving one trial out for each stimulus per fold, i.e., 10 trials left out per fold), for each participant the decoding accuracy was determined across time (Figure 2B). During cross validation, for each fold, decoders were trained on data of each 10 milliseconds time step and tested on left out data from the same time step. Therefore, decoding accuracy reflects the separability of the stimulus classes by the sensor values for each time step independently. Decoders were trained using a one-vs-all approach, which means that for each class, a separate classifier was trained using positive examples (target class) and negative examples (all other classes) plus null examples (data from before stimulus presentation, see below). This approach allows the decoder to provide independent estimates of detected events for each class.

For each participant, a final set of decoders (i.e., 10 decoders per participant, for each stimulus one decoder) were trained at 210 milliseconds after stimulus onset, a time point reflecting the average peak decoding time point computed for all participants. For the final decoders, data from before the auditory stimulus onset was added as a negative class with a ratio of 1:2, based upon results from previous publications reaching better sensitivity with higher negative class ratio (Y. Liu, Dolan, et al., 2021). Adding null data allows decoders to report low probabilities for all classes simultaneously in absence of a matching signal, and reduces false positives while retaining relative probabilities between true classes. Together with the use of a sparsity constraint on the logistic regression coefficients, this increases the sensitivity of sequence detection by reducing spatial correlations of decoder weights (see also Liu et al., 2021). For a visualization of relevant sensor positions, see Supplementary section of Kern et al., (2024). Decoders were then applied to the two resting state session data. This resulted in ten probability vectors across the resting state sessions, one for each item, in steps of 10 milliseconds. These probabilities indicate the similarity of the current sensor-level activity to the activity pattern elicited by exposure to the stimulus and can therefore be used as a proxy for detecting active representations, akin to a representational pattern analysis approach (RSA, Grootswagers et al., 2017).

Sequential replay analysis

To test whether individual items were reactivated in sequence at a particular time lag, we applied temporally delayed linear modelling (TDLM, Liu et al., 2021) to the resting state segments, using a Python implementation of the algorithm (TDLM-Python, Kern, 2024). In brief, the TDLM method approximates a time lagged cross-correlation of reactivation strength in the context of a particular

transition pattern, quantifying evidence for a certain activity transition pattern distributed in time. As input for the sequential analysis, we used the probabilities of the ten classifiers corresponding to the stimuli, which we normalized by dividing each class probability by the mean of all classes.

Using a linear model, the method first estimates evidence for sequential activation of the decoded item representations at different time lags. For each item i at each time lag Δt up to 300 milliseconds it estimates a linear model of form:

$$Y_i=Y(\Delta t)\times\beta_i(\Delta t)$$

where Y_i contains the decoded probability output of the classifier of item i and $Y(\Delta t)$ is simply Y time lagged by Δt. When solving this equation for $\beta_i(\Delta t)$ the predictive strength of $Y(\Delta t)$ for the occurrence of Y_i at each time lag Δt can be estimated. Calculated for each stimulus i, an empirical transition matrix $T_e(\Delta t)$ that indexes evidence for a transition of any item j to item i at time lag Δt can be created (i.e., a 10x10 transition matrix per time lag, each column j contains the predictive strength of j for each item i at time lag Δt). These matrices are then combined with a ground truth transition matrix T (encoding the valid sequence transitions of interest) by taking the Frobenius inner product. This returns a single value $Z_{\Delta t}$ for each time lag, indicating how strongly the detected transitions in the empirical data follow expected task transitions, which is termed “sequenceness”. Using different transition matrices to depict forward (T_f) and backward (T_b) replay, evidence for replay at different time lags for each trial is estimated separately. To control for auto-correlations of the signal, caused by large brain oscillations such as eyes-closed alpha(Y. Liu, Dolan, et al., 2021), we added time-shifted versions of the decoded probabilities to the GLM in 10 Hz intervals. This process is applied to each trial individually, and resulting sequenceness values are averaged to provide a final sequenceness value per participant for each time lag Δt. To test for statistical significance, a baseline distribution is sampled by permuting the rows of the transition matrix 1000 times (creating transition matrices with random transitions; identity-based permutation (Liu et al., 2021) and calculate sequenceness across all time lags for each permutation. The null distribution is then constructed by taking the peak sequenceness across all time lags for each permutation. To minimize possible participant-specific biases on the magnitude of sequenceness values, we z-scored along the time lag axis for each permutation, for each participant, similar as previously proposed (Wimmer et al., 2020).

Resting state analysis

To assess whether previously learned sequences are replayed during the resting state, we tested for significant sequenceness using the above-mentioned permutation test for forward and backward sequenceness. Additionally, we compared the sequenceness results to the control resting state by subtracting the sequenceness values on the participant level. Additionally to the maximum across all

permutations, we report the 95% confidence interval of the maxima across each permutation (Y. Liu, Dolan, et al., 2021). Finally, to assess if sequential replay was correlated with the participant's performance, we calculated a Pearson correlation between peak sequenceness across all time lags and the retrieval performance (as in Kern et al., 2024).

Parameter exploration

For completeness and transparency, we report what parameters we explored during the exploration phase on the first half of the data set (final results were calculated on a held-out portion of the resting state data). For classifiers, we tried Random Forest Classifiers, Support-Vector-Machines as well as LDA. We applied different normalizations of the MEG data by z-scoring the raw data along channels, times as well as across the entire recording. These were all inferior in terms of localizer decoding accuracy compared to the current approach. We trained on single time points and averaged time windows, including PCA. We employed z-scoring on the sequenceness values, on the probability estimates as well as using raw classifier outputs instead of probability estimates or normalizing each class by its mean probability. Nevertheless, after considering the vast space of possible parameters, we did not find alternative parameters that robustly showed a predicted replay pattern and thus, to avoid overfitting and remain comparable to the literature, we report this study with parameters most often used in previous research in terms of normalization, classifier choice (Logistic Regression) as well as training regimen. Crucially, these parameters were successfully applied by us to identify replay effects in our previous study using the retrieval data from this data set (Kern et al., 2024).

Exclusions

Replay analysis relies on a successive detection of stimuli, where the chance of detection exponentially decreases with each step (e.g., detecting two successive stimuli with a chance of 30% leaves a 9% chance of detecting a replay event). However, one needs to bear in mind that accuracy is a "winner-takes-all" metric indicating whether the top choice also has the highest probability, disregarding subtle, relative changes in assigned probability. As the methods used in this analysis are performed on probability estimates, and not class labels, one can expect that 30% is a rough lower bound and that the actual sensitivity within the analysis is higher. Additionally, based on pilot data, we found that attentive participants were able to reach 30% decodability, allowing its use as a data quality check. Therefore, we decided a priori that participants with a peak decoding accuracy of below 30% would be excluded from the analysis (nine participants in total), as obtained from the cross-validation of localizer trials. Additionally, as successful learning was necessary for the paradigm, we ensured all remaining participants had a retrieval performance of at least 50%. No participant had

more than 25% missed button presses, so no exclusion was necessary on this pre-registered criterion.

Methods Study II: Simulation

To better understand our null-finding, we conducted a simulation study. We applied a hybrid simulation approach, using resting state data recorded before any stimulus exposure as a sequence-free baseline, into which we inserted neural patterns taken from the localizer. By inserting these patterns at a specific time lag, we can create a ground truth of replay-like events that should be well-decodable. The advantage of using real-world MEG data over synthetic data is that it includes all nuisance confounders that might be present under realistic conditions, yet leaves room to control the variable of interest. Finally, by varying the density and length of inserted events, we can assess an upper bound of sensitivity of TDLM under optimal, yet realistic conditions.

Simulating replay by inserting localizer data into the control resting state

TDLM makes assumptions (implicit and explicit) about the underlying structure of replay. While it has yet to be shown these assumptions are based on the characteristics of actual replay, all methods pose other constraints (Cliff et al., 2023). Here, we aimed to create an optimal scenario tailored to TDLM. Therefore, we adhere to the following assumptions:

1. Individual items are reactivated and can be decoded throughout the recording
2. Individual item reactivations are brief, usually only of ~10-30 ms[1] duration
3. Item reactivations are non-random and adhere to a specific sequential pattern
4. A replay event comprises two or more reactivation events in close temporal proximity
5. There is a fixed time lag between all reactivations across all replay events

Additionally, we include the following constraints for the simulation

1. Classifiers trained on the peak time point of decodability of sensors from a localizer transfer well to reactivation events
2. Between each replay event (two or more stimulus reactivations), there is a refractory period of at least the time lag of interest in the analysis (i.e. 150 milliseconds)
3. Replay is correlated with memory performance during the retrieval session.
4. The replay density is stable across the recording.

[1] As for example shown in the replay example visualization in Figure 2 in Liu et al., (2019) or Figure 3 in Wimmer et al., (2020)

Based on these assumptions, we inserted replay events into the control resting state of each participant by first extracting stimulus-specific patterns of sensor activity and then added these patterns at sequential positions in the resting state. We created patterns by taking the mean sensor activation at the peak of decodability during the localizer of a specific class (as defined above, i.e. at 210 milliseconds). To isolate the stimulus-specific pattern from activity elicited by general sensory processing, we then subtracted the mean sensor values across all classes (akin to an event related potential of seeing any stimulus), for a visualization of the mean patterns across participants, see Supplement Figure 9. Next, we determined N replay onset points *t* throughout the resting state and inserted the pattern of a randomly chosen class by simply adding the pattern to the sensor values at time t_i. After a fixed time lag of 80 milliseconds after t_i, we inserted the pattern of the class that would follow according to the underlying sequence structure. We did not allow 150ms after and before each replay event from containing any other replay events, as this would have introduced interactions between two replay events within the used search window of 300ms. For simplicity, we only used one-step replay event transitions, i.e. containing two reactivation events.

Figure 8 shows the decoded probabilities at the timepoints *t* before and after addition of the stimulus-specific pattern. The target class is now well decodable, while other classes remain at a low baseline probability (Figure 8). Using this approach, we can simulate replay events while for the most part preserving other characteristics of the resting state in terms of endogenous oscillations that might introduce spurious sequenceness. However, note that this simulation approach is likely to slightly over-estimate decodability of reactivation events (which reflects in an average decoding accuracy of 43% after insertion which is higher than the decoding accuracy during the localizer). Additionally, as the classifier follows a one-versus-all classification approach it estimates probabilities for each class separately. Therefore, a small increase in probability can be seen even for non-target classes, which most probably stems from remaining patterns from general sensory processing and the slight increase in sensor magnitude after addition. Sensor values still follow the distribution of a naturalistic MEG signal after inserting patterns, i.e. are centred around zero and have a comparable standard deviation (see Supplement Figure 3).

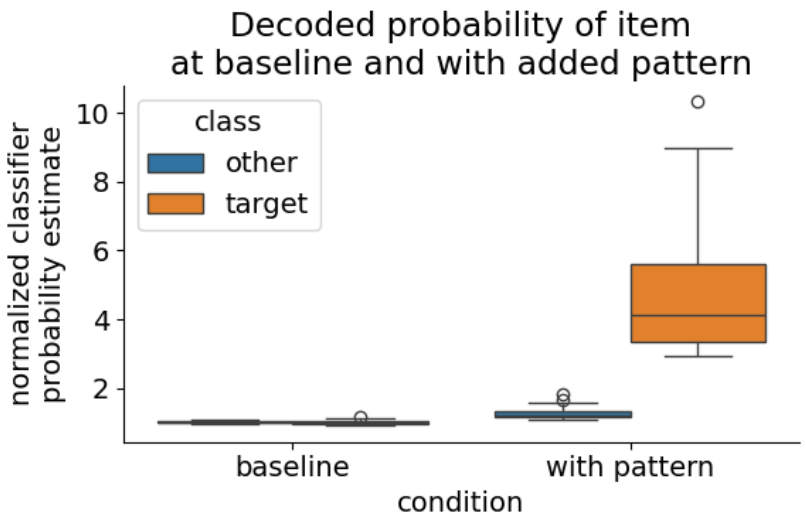

Figure 8 Normalized probability estimates of time points in the control resting state for the target class of which the pattern has been added and non-target class. Left: Time points at which no pattern has been inserted, both classes have a similar probability estimate at baseline. Right: At time points where the stimulus-specific pattern was added, the decoded probability estimate is significantly increased. Note that also the probability estimate of non-target classes is slightly increased at the timepoint of pattern insertion, which is due to slight shifts in sensor values that heightens all probabilities by a small amount.

Replay density

Unlike intracranial or cell recordings, TDLM does not per-se detect individual replay events, but given a specific transition pattern ascertains evidence for sequenceness over a period of time. Each in-sequence reactivation of two or more items increases the specific time lag's sequenceness value. Therefore, the sequenceness magnitude strongly relies on the underlying density of decoded replay events, which is usually denoted in events per minute or min^{-1}. To assess the sensitivity of TDLM, we incrementally increased the density up to a theoretical maximum of around 200 min^{-1}, as given by the time lag of 160 milliseconds plus the above-defined refractory period of 150 milliseconds. Additionally, as replay is seen as instrumental to memory consolidation, the density was linearly scaled with the participant's retrieval memory performance (e.g. a participant with 50% memory performance had at maximum 80 min^{-1} = 160 min^{-1} * 50% events inserted). Note that we deliberately overestimated the link between replay and memory performance which has been estimated to be as low as r=0.2 in humans (Schapiro et al., 2018).

Reactivation event length

It is unclear how long is the span of individual decodable reactivation events in the context of MEG decoding. In primates, sharp wave ripples (SWR), as a detectable proxy for a reactivation event, are usually searched for in the range of 20 to 200 milliseconds (A. A. Liu et al., 2022), while mostly found to range from 50 to 100 milliseconds (Buzsáki, 2015), hence each individual reactivation is much shorter. There is no report of decoded reactivation event lengths in the context of MEG, however, spans can be estimated from example illustrations given by previous studies, where they mostly span 10-30 milliseconds. Nevertheless, even if reactivation events are brief, there seems to be a waxing period, a peak and a waning period. Therefore, we simulated this process by extracting the item-specific pattern around the decoding accuracy peak and weighting it with a gaussian (sigma=1, i.e. item-specific pattern at 210 milliseconds +- 20 milliseconds was inserted into 50 milliseconds centred around the reactivation event marker in the resting state with the following weighting: [0.058, 0.24, 1, 0.24, 0.058].).

Data availability

MaxFiltered and anonymized MEG raw data are available at Zenodo in two parts: Localizer data is available as v1 of https://doi.org/10.5281/zenodo.8001755 (Kern, 2023). Resting state data is available as v2 of https://doi.org/10.5281/zenodo.15629081 (Kern, 2025).

Code availability

The code of the analysis as well as the experiment paradigm and the stimulus material is available at https://github.com/CIMH-Clinical-Psychology/DeSMRRest-TDLM-Simulation.

Supplement figures

For supplementary figures of this draft, see after references.

Acknowledgment

This research was supported by an Emmy-Noether research grant awarded to GBF by the DFG (FE1617/2-1) and a project grant by the DGSM as well as a doctoral scholarship of the German Academic Scholarship Foundation, both awarded to SK. Additionally, we want to thank the ZIPP core facility of the Central Institute of Mental Health for their generous support of the study.

References

Ablin, P., Cardoso, J.-F., & Gramfort, A. (2018). Faster Independent Component Analysis by Preconditioning With Hessian Approximations. *IEEE Transactions on Signal Processing*, *66*(15), 4040–4049. IEEE Transactions on Signal Processing. https://doi.org/10.1109/TSP.2018.2844203

Ambrose, R. E., Pfeiffer, B. E., & Foster, D. J. (2016). Reverse Replay of Hippocampal Place Cells Is Uniquely Modulated by Changing Reward. *Neuron*, *91*(5), 1124–1136. https://doi.org/10.1016/j.neuron.2016.07.047

Axmacher, N., Elger, C. E., & Fell, J. (2008). Ripples in the medial temporal lobe are relevant for human memory consolidation. *Brain*, *131*(7), 1806–1817. https://doi.org/10.1093/brain/awn103

Bezsudnova, Y., Quinn, A. J., Wynn, S. C., & Jensen, O. (2024). Spatiotemporal Properties of Common Semantic Categories for Words and Pictures. *Journal of Cognitive Neuroscience*, *36*(8), 1760–1769. https://doi.org/10.1162/jocn_a_02182

Born, J., & Wilhelm, I. (2012). System consolidation of memory during sleep. *Psychological Research*, *76*(2), 192–203. https://doi.org/10.1007/s00426-011-0335-6

Buhry, L., Azizi, A. H., & Cheng, S. (2011). Reactivation, replay, and preplay: How it might all fit together. *Neural Plasticity*, *2011*. https://doi.org/10.1155/2011/203462

Buzsáki, G. (2015). Hippocampal sharp wave-ripple: A cognitive biomarker for episodic memory and planning. *Hippocampus*, *25*(10), 1073–1188. https://doi.org/10.1002/hipo.22488

Chambers, C. D. (2020). Verification Reports: A new article type at Cortex. *Cortex*, *129*, A1–A3. https://doi.org/10.1016/j.cortex.2020.04.020

Chen, Y. Y., Aponik-Gremillion, L., Bartoli, E., Yoshor, D., Sheth, S. A., & Foster, B. L. (2021). Stability of ripple events during task engagement in human hippocampus. *Cell Reports*, *35*(13), 109304. https://doi.org/10.1016/j.celrep.2021.109304

Chen, Z., Zheng, H., Zhou, J., Zheng, L., Lin, P., Wang, H., Dolan, R., Behrens, T., & Liu, Y. (2024). *Interpreting Sleep Activity Through Neural Contrastive Learning* (S. 2024.09.25.615100). bioRxiv. https://doi.org/10.1101/2024.09.25.615100

Cliff, O. M., Bryant, A. G., Lizier, J. T., Tsuchiya, N., & Fulcher, B. D. (2023). Unifying pairwise interactions in complex dynamics. *Nature Computational Science*, *3*(10), 883–893. https://doi.org/10.1038/s43588-023-00519-x

Dafflon, J., F. Da Costa, P., Váša, F., Monti, R. P., Bzdok, D., Hellyer, P. J., Turkheimer, F., Smallwood, J., Jones, E., & Leech, R. (2022). A guided multiverse study of neuroimaging analyses. *Nature Communications*, *13*(1), 3758. https://doi.org/10.1038/s41467-022-31347-8

Delorme, A. (2022). *EEG is better left alone* [Preprint]. Neuroscience. https://doi.org/10.1101/2022.12.03.518987

Denis, D., Schapiro, A. C., Poskanzer, C., Bursal, V., Charon, L., Morgan, A., & Stickgold, R. (2020). The roles of item exposure and visualization success in the consolidation of memories across wake and sleep. *Learning & Memory*, *27*(11), 451–456. https://doi.org/10.1101/lm.051383.120

Deuker, L., Olligs, J., Fell, J., Kranz, T. A., Mormann, F., Montag, C., Reuter, M., Elger, C. E., & Axmacher, N. (2013). Memory Consolidation by Replay of Stimulus-Specific Neural Activity. *Journal of Neuroscience*, *33*(49), 19373–19383. https://doi.org/10.1523/JNEUROSCI.0414-13.2013

Diba, K., & Buzsáki, G. (2007). Forward and reverse hippocampal place-cell sequences during ripples. *Nature Neuroscience*, *10*(10), 1241–1242. https://doi.org/10.1038/nn1961

Diekelmann, S., & Born, J. (2010). The memory function of sleep. *Nature Reviews Neuroscience*, *11*(2), 114–126. https://doi.org/10.1038/nrn2762

Dijkstra, N., Bosch, S. E., & Gerven, M. A. J. van. (2019). Shared Neural Mechanisms of Visual Perception and Imagery. *Trends in Cognitive Sciences*, *23*(5), 423–434. https://doi.org/10.1016/j.tics.2019.02.004

Dijkstra, N., Gaal, S. van, Geerligs, L., Bosch, S. E., & Gerven, M. A. J. van. (2021). No Evidence for Neural Overlap between Unconsciously Processed and Imagined Stimuli. *eNeuro*, *8*(5). https://doi.org/10.1523/ENEURO.0228-21.2021

Drosopoulos, S., Schulze, C., Fischer, S., & Born, J. (2007). Sleep's function in the spontaneous recovery and consolidation of memories. *Journal of Experimental Psychology. General*, *136*(2), 169–183. https://doi.org/10.1037/0096-3445.136.2.169

Eichenlaub, J.-B., Jarosiewicz, B., Saab, J., Franco, B., Kelemen, J., Halgren, E., Hochberg, L. R., & Cash, S. S. (2020). Replay of Learned Neural Firing Sequences during Rest in Human Motor Cortex. *Cell Reports*, *31*(5), 107581. https://doi.org/10.1016/j.celrep.2020.107581

Eldar, E., Lièvre, G., Dayan, P., & Dolan, R. J. (2020). The roles of online and offline replay in planning. *eLife*, *9*, e56911. https://doi.org/10/gms5sp

Engel, A. K., Moll, C. K. E., Fried, I., & Ojemann, G. A. (2005). Invasive recordings from the human brain: Clinical insights and beyond. *Nature Reviews Neuroscience*, *6*(1), Article 1. https://doi.org/10.1038/nrn1585

Eschenko, O., Ramadan, W., Mölle, M., Born, J., & Sara, S. J. (2008a). Sustained increase in hippocampal sharp-wave ripple activity during slow-wave sleep after learning. *Learning & Memory*, *15*(4), 222–228. https://doi.org/10.1101/lm.726008

Eschenko, O., Ramadan, W., Mölle, M., Born, J., & Sara, S. J. (2008b). Sustained increase in hippocampal sharp-wave ripple activity during slow-wave sleep after learning. *Learning & Memory*, *15*(4), 222. https://doi.org/10.1101/lm.726008

Feld, G. B., Bernard, M., Rawson, A. B., & Spiers, H. J. (2022). Sleep targets highly connected global and local nodes to aid consolidation of learned graph networks. *Scientific Reports*, *12*(1), Article 1. https://doi.org/10.1038/s41598-022-17747-2

Feld, G. B., & Born, J. (2017). Sculpting memory during sleep: Concurrent consolidation and forgetting. *Current Opinion in Neurobiology*, *44*, 20–27. https://doi.org/10/gbrvqm

Feld, G. B., & Born, J. (2020). Neurochemical mechanisms for memory processing during sleep: Basic findings in humans and neuropsychiatric implications. *Neuropsychopharmacology*, 1–14. https://doi.org/10.1038/s41386-019-0490-9

Feld, G. B., Lange, T., Gais, S., & Born, J. (2013). Sleep-Dependent Declarative Memory Consolidation—Unaffected after Blocking NMDA or AMPA Receptors but Enhanced by NMDA Coagonist D -Cycloserine. *Neuropsychopharmacology*, *38*(13), Article 13. https://doi.org/10.1038/npp.2013.179

Fell, J., & Axmacher, N. (2011). The role of phase synchronization in memory processes. *Nature Reviews Neuroscience*, *12*(2), 105–118. https://doi.org/10.1038/nrn2979

Findlay, G., Tononi, G., & Cirelli, C. (2020). The evolving view of replay and its functions in wake and sleep. *SLEEP Advances*, *1*(1), zpab002. https://doi.org/10.1093/sleepadvances/zpab002

Foster, D. J. (2017). Replay Comes of Age. *Annual Review of Neuroscience*, *40*(1), 581–602. https://doi.org/10.1146/annurev-neuro-072116-031538

Foster, D. J., & Wilson, M. A. (2006). Reverse replay of behavioural sequences in hippocampal place cells during the awake state. *Nature*, *440*(7084), 680–683. https://doi.org/10.1038/nature04587

Galer, S., Urbain, C., De Tiège, X., Emeriau, M., Leproult, R., Deliens, G., Nonclerq, A., Peigneux, P., & Van Bogaert, P. (2015). Impaired sleep-related consolidation of declarative memories in idiopathic focal epilepsies of childhood. *Epilepsy & Behavior*, *43*, 16–23. https://doi.org/10.1016/j.yebeh.2014.11.032

Genzel, L., Dragoi, G., Frank, L., Ganguly, K., de la Prida, L., Pfeiffer, B., & Robertson, E. (2020). A consensus statement: Defining terms for reactivation analysis. *Philosophical Transactions of the Royal Society B: Biological Sciences*, *375*(1799), 20200001. https://doi.org/10.1098/rstb.2020.0001

Gramfort, A. (2013). MEG and EEG data analysis with MNE-Python. *Frontiers in Neuroscience*, *7*. https://doi.org/10.3389/fnins.2013.00267

Grootswagers, T., Wardle, S. G., & Carlson, T. A. (2017). Decoding Dynamic Brain Patterns from Evoked Responses: A Tutorial on Multivariate Pattern Analysis Applied to Time Series Neuroimaging Data. *Journal of Cognitive Neuroscience*, *29*(4), 677–697. https://doi.org/10.1162/jocn_a_01068

Hall, E. L., Robson, S. E., Morris, P. G., & Brookes, M. J. (2014). The relationship between MEG and fMRI. *NeuroImage*, *102*, 80–91. https://doi.org/10.1016/j.neuroimage.2013.11.005

Hasselmo, M. E., Bodelón, C., & Wyble, B. P. (2002). A Proposed Function for Hippocampal Theta Rhythm: Separate Phases of Encoding and Retrieval Enhance Reversal of Prior Learning. *Neural Computation*, *14*(4), 793–817. https://doi.org/10.1162/089976602317318965

Higgins, C., Liu, Y., Vidaurre, D., Kurth-Nelson, Z., Dolan, R., Behrens, T., & Woolrich, M. (2021). Replay bursts in humans coincide with activation of the default mode and parietal alpha networks. *Neuron*, *109*(5), 882-893.e7. https://doi.org/10.1016/j.neuron.2020.12.007

Hoddes, E., Zarcone, V., Smythe, H., Phillips, R., & Dement, W. C. (1973). Quantification of Sleepiness: A New Approach. *Psychophysiology*, *10*(4), 431–436. https://doi.org/10.1111/j.1469-8986.1973.tb00801.x

Hoffman, K. L., Dragan, M. C., Leonard, T. K., Micheli, C., Montefusco-Siegmund, R., & Valiante, T. A. (2013). Saccades during visual exploration align hippocampal 3–8 Hz rhythms in human and non-human primates. *Frontiers in Systems Neuroscience*, *7*. https://doi.org/10.3389/fnsys.2013.00043

Hoffman, K. L., & McNaughton, B. L. (2002). Coordinated reactivation of distributed memory traces in primate neocortex. *Science*, *297*(5589), 2070–2073. https://doi.org/10.1126/science.1073538

Huang, Q., & Luo, H. (2023). Shared structure facilitates working memory of multiple sequences via neural replay. *eLife*, *12*. https://doi.org/10.7554/eLife.93158.1

Huang, Q., Xiao, Z., Yu, Q., Luo, Y., Xu, J., Qu, Y., Dolan, R., Behrens, T., & Liu, Y. (2024). Replay-triggered brain-wide activation in humans. *Nature Communications*, *15*(1), 7185. https://doi.org/10.1038/s41467-024-51582-5

Huang, W., Yan, H., Wang, C., Li, J., Yang, X., Li, L., Zuo, Z., Zhang, J., & Chen, H. (2020). Long short-term memory-based neural decoding of object categories evoked by natural images. *Human Brain Mapping*, *February*, 1–12. https://doi.org/10.1002/hbm.25136

Huelin Gorriz, M., Takigawa, M., & Bendor, D. (2023). The role of experience in prioritizing hippocampal replay. *Nature Communications*, *14*(1), 8157. https://doi.org/10.1038/s41467-023-43939-z

Hughes, J. R. (1995). The Phenomenon of Travelling Waves: A Review. *Clinical Electroencephalography*, *26*(1), 1–6. https://doi.org/10.1177/155005949502600103

Humiston, G. B., Tucker, M. A., Summer, T., & Wamsley, E. J. (2019). Resting States and Memory Consolidation: A Preregistered Replication and Meta-Analysis. *Scientific Reports*, *9*(1), 19345. https://doi.org/10.1038/s41598-019-56033-6

Jas, M., Engemann, D. A., Bekhti, Y., Raimondo, F., & Gramfort, A. (2017). Autoreject: Automated artifact rejection for MEG and EEG data. *NeuroImage*, *159*, 417–429. https://doi.org/10.1016/j.neuroimage.2017.06.030

Jiang, H., Liu, S., Geng, X., Caccavano, A., Conant, K., Vicini, S., & Wu, J. (2018). Pacing Hippocampal Sharp-Wave Ripples With Weak Electric Stimulation. *Frontiers in Neuroscience*, *12*, 164. https://doi.org/10.3389/fnins.2018.00164

Jiang, X., Gonzalez-Martinez, J., Cash, S. S., Chauvel, P., Gale, J., & Halgren, E. (2020). Improved identification and differentiation from epileptiform activity of human hippocampal sharp wave ripples during NREM sleep. *Hippocampus*, *30*(6), 610–622. https://doi.org/10.1002/hipo.23183

Joo, H. R., & Frank, L. M. (2018). The hippocampal sharp wave-ripple in memory retrieval for immediate use and consolidation. *Nature Reviews. Neuroscience*, *19*(12), 744. https://doi.org/10.1038/s41583-018-0077-1

Kanak, D. J., Rose, G. M., Zaveri, H. P., & Patrylo, P. R. (2013). Altered Network Timing in the CA3-CA1 Circuit of Hippocampal Slices from Aged Mice. *PLOS ONE*, *8*(4), e61364. https://doi.org/10.1371/journal.pone.0061364

Kern, S. (2003). *Reactivation strength during cued recall is modulated by graph distance within cognitive maps* (Version v1) [Dataset]. Zenodo. https://doi.org/10.5281/zenodo.8001754

Kern, S. (2024). *skjerns/TDLM-Python: V0.1 Temporally Delayed Linear Modelling for Python* (Version v0.1) [Software]. Zenodo. https://doi.org/10.5281/zenodo.12623445

Kern, S. (2025). *Challenges in Replay Detection by TDLM in Post-Encoding Resting State* [Dataset]. Zenodo. https://doi.org/10.5281/zenodo.15629081

Kern, S., Nagel, J., Gerchen, M. F., Gürsoy, Ç., Meyer-Lindenberg, A., Kirsch, P., Dolan, R. J., Gais, S., & Feld, G. B. (2024). Reactivation strength during cued recall is modulated by graph distance within cognitive maps. *eLife*, *12*, RP93357. https://doi.org/10.7554/eLife.93357

Kerrén, C., Linde-Domingo, J., Hanslmayr, S., & Wimber, M. (2018). An Optimal Oscillatory Phase for Pattern Reactivation during Memory Retrieval. *Current Biology*, *28*(21), 3383-3392.e6. https://doi.org/10.1016/j.cub.2018.08.065

Kerrén, C., van Bree, S., Griffiths, B. J., & Wimber, M. (2022). Phase separation of competing memories along the human hippocampal theta rhythm. *eLife*, *11*, e80633. https://doi.org/10.7554/eLife.80633

Klinzing, J. G., Niethard, N., & Born, J. (2019). Mechanisms of systems memory consolidation during sleep. *Nature Neuroscience*, *22*(10), 1598–1610. https://doi.org/10.1038/s41593-019-0467-3

Komsky, J. C. (2015). Conscious replay during rest and relational processing. *PhD Thesis*.

Kragel, J. E., VanHaerents, S., Templer, J. W., Schuele, S., Rosenow, J. M., Nilakantan, A. S., & Bridge, D. J. (2020). Hippocampal theta coordinates memory processing during visual exploration. *eLife*, *9*, e52108. https://doi.org/10.7554/eLife.52108

Kriegeskorte, N., Simmons, W. K., Bellgowan, P. S. F., & Baker, C. I. (2009). Circular analysis in systems neuroscience: The dangers of double dipping. *Nature Neuroscience*, *12*(5), 535–540. https://doi.org/10.1038/nn.2303

Kurth-Nelson, Z., Economides, M., Dolan, R. J., & Dayan, P. (2016). Fast Sequences of Non-spatial State Representations in Humans. *Neuron*, *91*(1), 194–204. https://doi.org/10.1016/j.neuron.2016.05.028

Lee, A. K., & Wilson, M. A. (2002). Memory of Sequential Experience in the Hippocampus during Slow Wave Sleep. *Neuron*, *36*(6), 1183–1194. https://doi.org/10.1016/S0896-6273(02)01096-6

Liu, A. A., Henin, S., Abbaspoor, S., Bragin, A., Buffalo, E. A., Farrell, J. S., Foster, D. J., Frank, L. M., Gedankien, T., Gotman, J., Guidera, J. A., Hoffman, K. L., Jacobs, J., Kahana, M. J., Li, L., Liao, Z., Lin, J. J., Losonczy, A., Malach, R., … Buzsáki, G. (2022). A consensus statement on detection of hippocampal sharp wave ripples and differentiation from other fast oscillations. *Nature Communications*, *13*(1), 6000. https://doi.org/10.1038/s41467-022-33536-x

Liu, Y., Dolan, R. J., Higgins, C., Penagos, H., Woolrich, M. W., Ólafsdóttir, H. F., Barry, C., Kurth-Nelson, Z., & Behrens, T. E. (2021). Temporally delayed linear modelling (TDLM) measures replay in both animals and humans. *eLife*, *10*, e66917. https://doi.org/10/gkf6sk

Liu, Y., Dolan, R. J., Kurth-Nelson, Z., & Behrens, T. E. J. (2019). Human Replay Spontaneously Reorganizes Experience. *Cell*, *178*(3), 640-652.e14. https://doi.org/10.1016/j.cell.2019.06.012

Liu, Y., Mattar, M. G., Behrens, T. E. J., Daw, N. D., & Dolan, R. J. (2021). Experience replay is associated with efficient nonlocal learning. *Science*, *372*(6544), eabf1357. https://doi.org/10.1126/science.abf1357

Liu, Y., Nour, M. M., Schuck, N. W., Behrens, T. E. J., & Dolan, R. J. (2022). Decoding cognition from spontaneous neural activity. *Nature Reviews Neuroscience*. https://doi.org/10/gppd4d

Mallory, C. S., Widloski, J., & Foster, D. J. (2025). The time course and organization of hippocampal replay. *Science*, *387*(6733), 541–548. https://doi.org/10.1126/science.ads4760

McFadyen, J., Liu, Y., & Dolan, R. J. (2023). Differential replay of reward and punishment paths predicts approach and avoidance. *Nature Neuroscience*, *26*(4), Article 4. https://doi.org/10.1038/s41593-023-01287-7

Muller, L., Chavane, F., Reynolds, J., & Sejnowski, T. J. (2018). Cortical travelling waves: Mechanisms and computational principles. *Nature Reviews Neuroscience*, *19*(5), 255–268. https://doi.org/10.1038/nrn.2018.20

Nádasdy, Z., Hirase, H., Czurkó, A., Csicsvari, J., & Buzsáki, G. (1999). Replay and Time Compression of Recurring Spike Sequences in the Hippocampus. *The Journal of Neuroscience*, *19*(21), 9497–9507. https://doi.org/10.1126/science.1182395

Ngo, H.-V., Fell, J., & Staresina, B. (2020). Sleep spindles mediate hippocampal-neocortical coupling during long-duration ripples. *eLife*, *9*, e57011. https://doi.org/10.7554/eLife.57011

Norman, Y., Yeagle, E. M., Khuvis, S., Harel, M., Mehta, A. D., & Malach, R. (2019). Hippocampal sharp-wave ripples linked to visual episodic recollection in humans. *Science*, *365*(6454), eaax1030. https://doi.org/10.1126/science.aax1030

Nour, M. M., Liu, Y., Arumuham, A., Kurth-Nelson, Z., & Dolan, R. J. (2021). Impaired neural replay of inferred relationships in schizophrenia. *Cell*, *184*(16), 4315-4328.e17. https://doi.org/10/gmcq6d

Nour, M. M., Liu, Y., Higgins, C., Woolrich, M. W., & Dolan, R. J. (2023). Reduced coupling between offline neural replay events and default mode network activation in schizophrenia. *Brain Communications*, *5*(2), fcad056. https://doi.org/10.1093/braincomms/fcad056

Ogawa, K., Yang, Y., Yang, H., Imai, F., & Imamizu, H. (2024). *Human sensorimotor cortex reactivates recent visuomotor experience during awake rest*. https://doi.org/10.1101/2024.05.26.595974

O'Keefe, J. (1976). Place units in the hippocampus of the freely moving rat. *Experimental Neurology*, *51*(1), 78–109. https://doi.org/10.1016/0014-4886(76)90055-8

Pavlides, C., & Winson, J. (1989). Influences of hippocampal place cell firing in the awake state on the activity of these cells during subsequent sleep episodes. *The Journal of Neuroscience*, *9*(8), 2907–2918. https://doi.org/10.1523/JNEUROSCI.09-08-02907.1989

Payne, J. D., Tucker, M. A., Ellenbogen, J. M., Wamsley, E. J., Walker, M. P., Schacter, D. L., & Stickgold, R. (2012). Memory for Semantically Related and Unrelated Declarative Information: The Benefit of Sleep, the Cost of Wake. *PLOS ONE*, *7*(3), e33079. https://doi.org/10.1371/journal.pone.0033079

Pedregosa, F., Varoquaux, G., Gramfort, A., Michel, V., Thirion, B., Grisel, O., Blondel, M., Prettenhofer, P., Weiss, R., Dubourg, V., Vanderplas, J., Passos, A., Cournapeau, D., Brucher, M., Perrot, M., & Duchesnay, É. (2011). Scikit-learn: Machine Learning in Python. *Journal of Machine Learning Research*, *12*(85), 2825–2830.

Ponomarenko, A. A., Lin, J.-S., Selbach, O., & Haas, H. L. (2003). Temporal pattern of hippocampal high-frequency oscillations during sleep after stimulant-evoked waking. *Neuroscience*, *121*(3), 759–769. https://doi.org/10.1016/S0306-4522(03)00524-4

Rasch, B. H., Born, J., & Gais, S. (2006). Combined Blockade of Cholinergic Receptors Shifts the Brain from Stimulus Encoding to Memory Consolidation. *Journal of Cognitive Neuroscience*, *18*(5), 793–802. Journal of Cognitive Neuroscience. https://doi.org/10.1162/jocn.2006.18.5.793

Rossion, B., & Pourtois, G. (2001). Revisiting snodgrass and Vanderwart's object database: Color and texture improve object recognition. *Journal of Vision*, *1*(3), 413. https://doi.org/10.1167/1.3.413

Roumis, D. K., & Frank, L. M. (2015). Hippocampal sharp-wave ripples in waking and sleeping states. *Current Opinion in Neurobiology*, *35*, 6–12. https://doi.org/10.1016/j.conb.2015.05.001

Schapiro, A. C., McDevitt, E. A., Rogers, T. T., Mednick, S. C., & Norman, K. A. (2018). Human hippocampal replay during rest prioritizes weakly learned information and predicts memory performance. *Nature Communications*, *9*(1), Article 1. https://doi.org/10.1038/s41467-018-06213-1

Schlichting, M. L., & Preston, A. R. (2014). Memory reactivation during rest supports upcoming learning of related content. *Proceedings of the National Academy of Sciences*, *111*(44), 15845–15850. https://doi.org/10.1073/pnas.1404396111

Schreiner, T., Griffiths, B. J., Kutlu, M., Vollmar, C., Kaufmann, E., Quach, S., Remi, J., Noachtar, S., & Staudigl, T. (2024). Spindle-locked ripples mediate memory reactivation during human NREM sleep. *Nature Communications*, *15*(1), 5249. https://doi.org/10.1038/s41467-024-49572-8

Schreiner, T., Petzka, M., Staudigl, T., & Staresina, B. P. (2021). Endogenous memory reactivation during sleep in humans is clocked by slow oscillation-spindle complexes. *Nature Communications*, *12*(1), 3112. https://doi.org/10/gkgmkx

Schuck, N. W., & Niv, Y. (2019). Sequential replay of nonspatial task states in the human hippocampus. *Science*, *364*(6447). https://doi.org/10.1126/science.aaw5181

Schwartenbeck, P., Baram, A., Liu, Y., Mark, S., Muller, T., Dolan, R., Botvinick, M., Kurth-Nelson, Z., & Behrens, T. (2023). Generative replay underlies compositional inference in the hippocampal-prefrontal circuit. *Cell*, *186*(22), 4885-4897.e14. https://doi.org/10.1016/j.cell.2023.09.004

Seow, T. X. F., McFadyen, J., Dolan, R. J., & Hauser, T. U. (2024). *Excessive neural replay of aversive and uncertain options predicts human irrational decision-making*.

Staresina, B. P., Bergmann, T. O., Bonnefond, M., van der Meij, R., Jensen, O., Deuker, L., Elger, C. E., Axmacher, N., & Fell, J. (2015). Hierarchical nesting of slow oscillations, spindles and ripples in the human hippocampus during sleep. *Nature Neuroscience*, *18*(11), Article 11. https://doi.org/10.1038/nn.4119

Staresina, B. P., Henson, R. N. A., Kriegeskorte, N., & Alink, A. (2012). Episodic Reinstatement in the Medial Temporal Lobe. *Journal of Neuroscience*, *32*(50), 18150–18156. https://doi.org/10.1523/JNEUROSCI.4156-12.2012

Tambini, A., & Davachi, L. (2013). Persistence of hippocampal multivoxel patterns into postencoding rest is related to memory. *Proceedings of the National Academy of Sciences*, *110*(48), 19591–19596. https://doi.org/10.1073/pnas.1308499110

Tambini, A., Ketz, N., & Davachi, L. (2010). Enhanced Brain Correlations during Rest Are Related to Memory for Recent Experiences. *Neuron*, *65*(2), 280–290. https://doi.org/10.1016/j.neuron.2010.01.001

Taulu, S., & Simola, J. (2006). Spatiotemporal signal space separation method for rejecting nearby interference in MEG measurements. *Physics in Medicine and Biology*, *51*(7), 1759–1768. https://doi.org/10/b5bjqg

van Diepen, R. M., & Mazaheri, A. (2018). The Caveats of observing Inter-Trial Phase-Coherence in Cognitive Neuroscience. *Scientific Reports*, *8*(1), 2990. https://doi.org/10.1038/s41598-018-20423-z

Wamsley, E. J. (2022). Offline memory consolidation during waking rest. *Nature Reviews Psychology*, *1*(8), 441–453. https://doi.org/10.1038/s44159-022-00072-w

Watrous, A. J., Deuker, L., Fell, J., & Axmacher, N. (2015). Phase-amplitude coupling supports phase coding in human ECoG. *eLife*, *4*, e07886. https://doi.org/10.7554/eLife.07886

Watson, D., Clark, L. A., & Tellegen, A. (1988). Development and validation of brief measures of positive and negative affect: The PANAS scales. *Journal of Personality and Social Psychology*, *54*(6), 1063–1070. https://doi.org/10.1037/0022-3514.54.6.1063

Wiegand, J.-P. L., Gray, D. T., Schimanski, L. A., Lipa, P., Barnes, C. A., & Cowen, S. L. (2016). Age Is Associated with Reduced Sharp-Wave Ripple Frequency and Altered Patterns of Neuronal Variability. *The Journal of Neuroscience*, *36*(20), 5650–5660. https://doi.org/10.1523/JNEUROSCI.3069-15.2016

Wilson, M. A., & McNaughton, B. L. (1994). Reactivation of Hippocampal Ensemble Memories During Sleep. *Science*, *265*(5172), 676–679. https://doi.org/10.1126/science.8036517

Wimmer, G. E., Liu, Y., McNamee, D. C., & Dolan, R. J. (2023). Distinct replay signatures for prospective decision-making and memory preservation. *Proceedings of the National Academy of Sciences*, *120*(6), e2205211120. https://doi.org/10.1073/pnas.2205211120

Wimmer, G. E., Liu, Y., Vehar, N., Behrens, T. E. J., & Dolan, R. J. (2020). Episodic memory retrieval success is associated with rapid replay of episode content. *Nature Neuroscience*, *23*(8), Article 8. https://doi.org/10.1038/s41593-020-0649-z

Wise, T., Liu, Y., Chowdhury, F., & Dolan, R. J. (2021). Model-based aversive learning in humans is supported by preferential task state reactivation. *Science Advances*, *7*(31), eabf9616. https://doi.org/10.1126/sciadv.abf9616

Wittkuhn, L., Krippner, L. M., Koch, C., & Schuck, N. W. (2024). *Replay in Human Visual Cortex is Linked to the Formation of Successor Representations and Independent of Consciousness* (S. 2022.02.02.478787). bioRxiv. https://doi.org/10.1101/2022.02.02.478787

Wittkuhn, L., & Schuck, N. W. (2021). Dynamics of fMRI patterns reflect sub-second activation sequences and reveal replay in human visual cortex. *Nature Communications*, *12*(1), 1795. https://doi.org/10/gjhf54

Xiao, Q., Lu, M., Zhang, X., Guan, J., Li, X., Wen, R., Wang, N., Qian, L., Liao, Y., Zhang, Z., Liao, X., Jiang, C., Yue, F., Ren, S., Xia, J., Hu, J., Luo, F., Hu, Z., & He, C. (2024). Isolated theta waves originating from the midline thalamus trigger memory reactivation during NREM sleep in mice. *Nature Communications*, *15*(1), 9231. https://doi.org/10.1038/s41467-024-53522-9

Yu, Q., Luo, Y., Dolan, R., Ou, J., Huang, C., Wang, H., Xiao, Z., & Liu, Y. (2023). *Reduced Reverse Replay in Anxious Individuals Impairs Reward Prediction* (S. 2023.06.21.546031). bioRxiv. https://doi.org/10.1101/2023.06.21.546031

Zhang, H., Fell, J., & Axmacher, N. (2018). Electrophysiological mechanisms of human memory consolidation. *Nature Communications*, *9*(1), 4103. https://doi.org/10.1038/s41467-018-06553-y

Zhang, H., Fell, J., Staresina, B. P., Weber, B., Elger, C. E., & Axmacher, N. (2015). Gamma Power Reductions Accompany Stimulus-Specific Representations of Dynamic Events. *Current Biology*, *25*(5), 635–640. https://doi.org/10.1016/j.cub.2015.01.011

Zhou, Z., Kahana, M. J., & Schapiro, A. C. (2024). A unifying account of replay as context-driven memory reactivation. *eLife*, *13*. https://doi.org/10.7554/eLife.99931.1

Supplement

Which pattern to extract from the localizer

To extract a suitable pattern that can be added to the control resting state, some constraints need to be addressed. First, the pattern should elicit an increase in probability specific to the target class when added to the resting state data. Consequently, all non-target classes should not increase significantly compared to baseline. Because, if the baseline probability is increased, spurious sequenceness will occur simply due to the baseline increase, as is the case with oscillatory confounders (Y. Liu, Dolan, et al., 2021). Additionally, classifiers will also react to any event-locked visual activity, slightly increasing the probability of the target class, even if seeing an unrelated image. We initially elicited these patterns by taking the mean ERP per class adding the sensor values of the peak decoding time point to resting state positions. However, this shifted the distribution of sensor values in such a way that the baseline probability of non-target-classes also increased (Figure 8). Therefore, we opted to refine the pattern by taking the ERP of all other classes and subtracting it from the ERP of the target class. This has the advantage that it removes most of the background visual activity and only keeps activity specific to the target class.

Supplement Figures

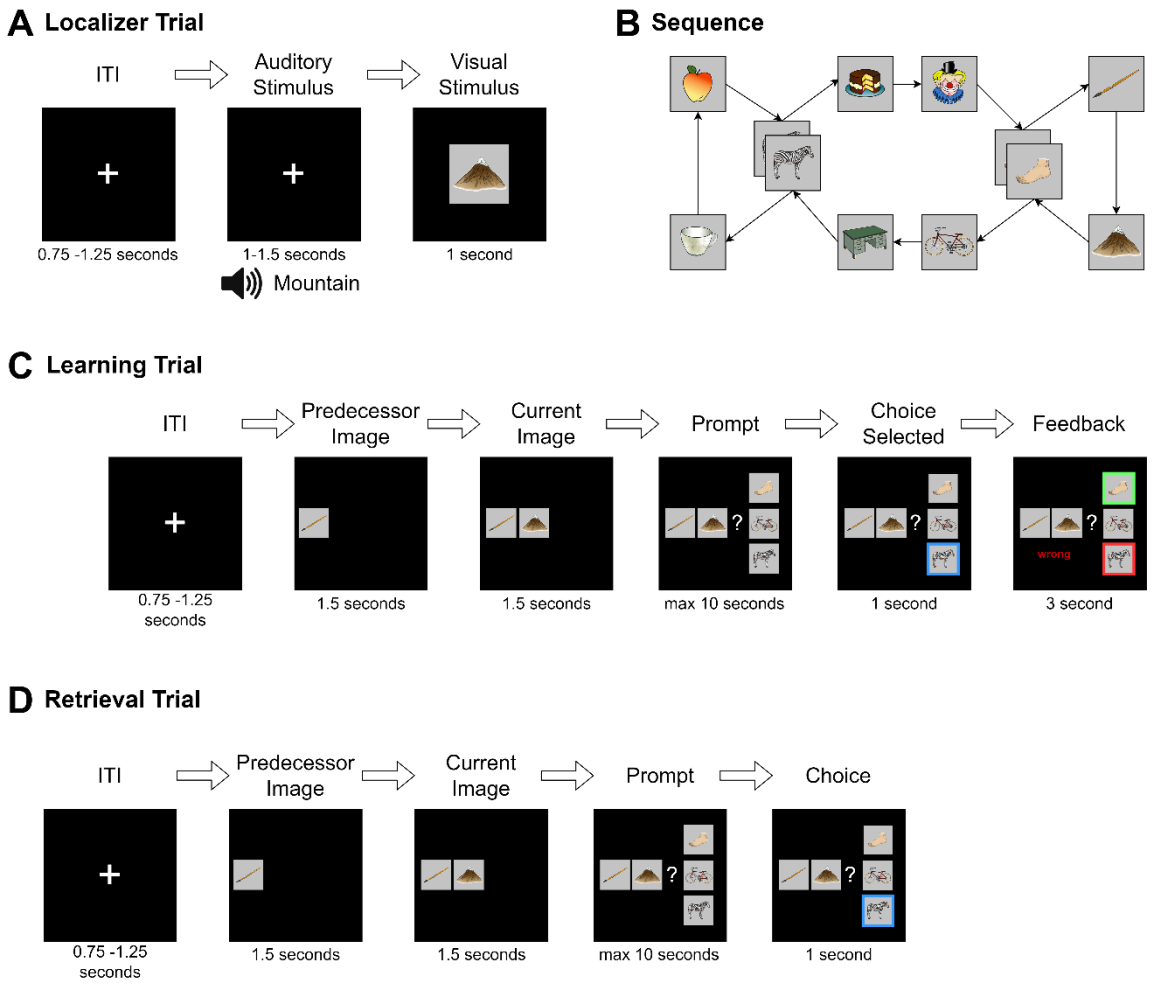

Supplement Figure 1 Detailed overview of the experiment procedure. A) During the localizer task, a word describing the stimulus was played via headphones and the corresponding visual item was then shown to the participant. In 4% of trials, the audio and visual cue did not match and in this case, participants were instructed to press a button on detection (to sustain attention to the stimuli and check for inattention). B) Graph layout of the task. Two elements could appear in two different triplets. The graph was directed such that each tuple had exactly one successor (e.g., apple→zebra could only be followed by cake and not mug), but individual items could have different successors (zebra alone could be followed by mug or cake). Participants never saw the illustrated birds-eye-view. C) During learning, in each trial one node was randomly chosen as the current node. First, its predecessor node was shown, followed by the current node with the participant then given a choice of three items. They were then required to choose the node that followed the displayed cue tuple. Feedback was then provided to the participant. This process was repeated until the participant reached 80% accuracy for any block or reached a maximum of six blocks of learning. D) The retrieval followed the same structure as the learning task, except that no feedback was given.

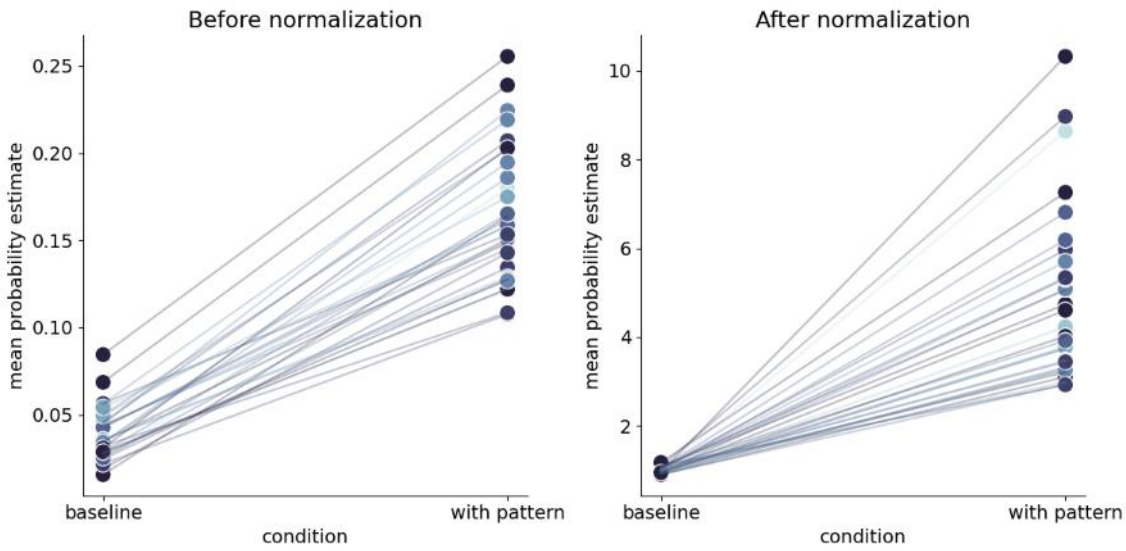

1190

Supplement Figure 2 Mean classifier probabilities before and after normalization, per participant for time points selected for replay pattern insertion. Left: Variance in baseline probability estimates can already be seen before pattern insertion, i.e. for some participants a higher baseline is present that for others. This higher baseline probability values (or rather their stronger absolute fluctuation) will lead to falsely increased sequenceness values in the GLM betas. Right: After normalization, baseline probabilities are similar across all participants. Blue shading indicates the participant's performance with lighter shading at 50% and darkest shading at 100% memory performance.

1191

1192

1193

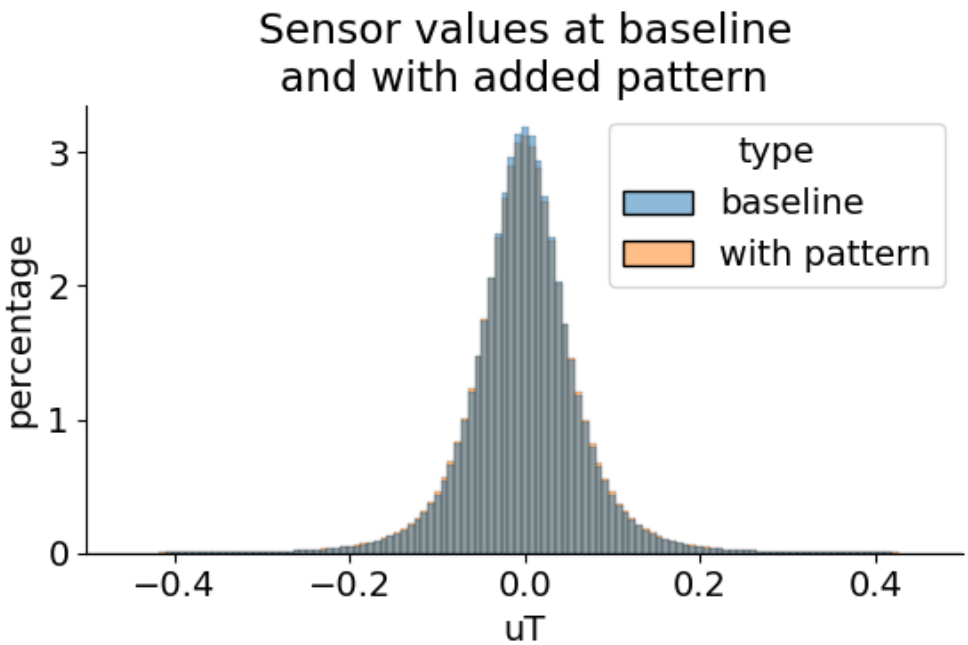

1194

Supplement Figure 3 Distribution of raw sensor values before and after insertion of the simulation pattern. As MEG measures differences in magnetic field strength, the signal is centred on zero. Adding

a pattern that is extracted from a zero-centred distribution should not affect the distributions mean and hence still produce a valid MEG signal, which is shown in the figure. However, a very small difference in spread between the two distribution can be seen, indicating that sensor values are not exactly following the same distribution characteristics after adding the stimulus-specific pattern, which might explain the small increase in baseline probability for non-target classes in Figure 8.

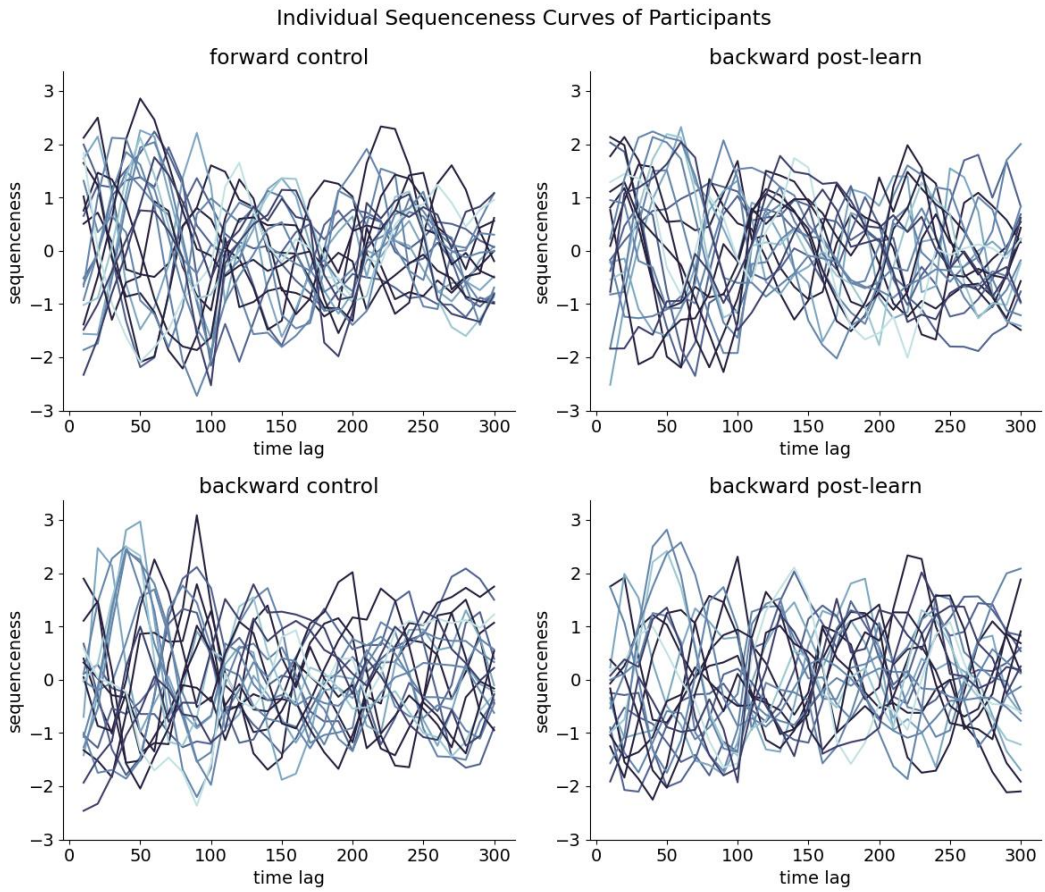

Supplement Figure 4 Individual sequenceness curves for all participants in the control resting state (left) and the post-learning resting state (right), for forward (upper), and backward sequenceness (bottom). The participant's performance is indicated in shades of blue, from the lightest shade at 50% to the darkest shade at 100% retrieval performance. Note that there is an oscillatory component present in all sequenceness curves, however, their phase and exact amplitude seems to be shifted.

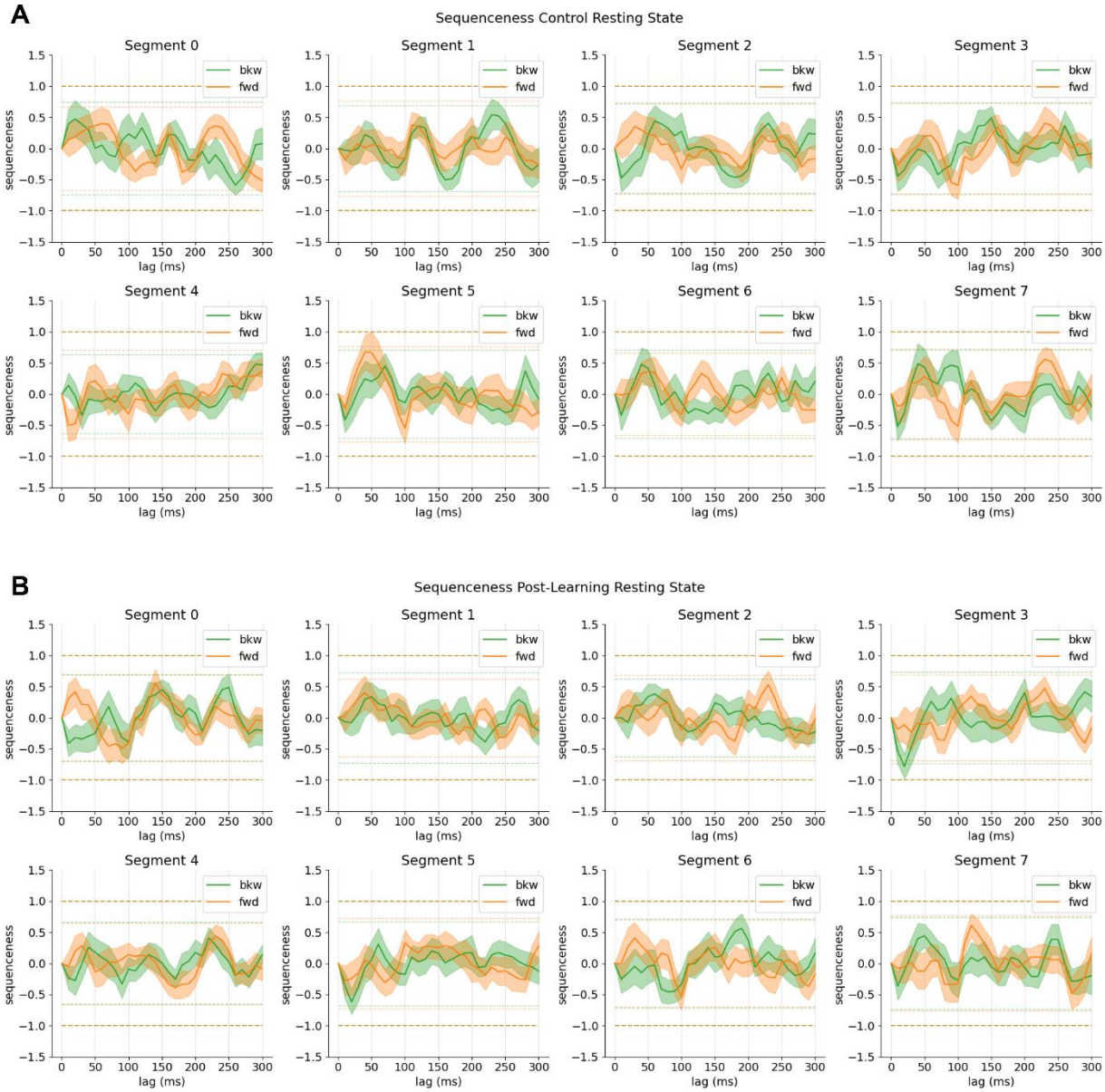

Supplement Figure 5 Individual sequenceness curves for different segments of A) control resting state and B) post-learning resting state. Each segment is taken from minute N of the respective resting state. For each participant, from each segment either the first or second 30-second interval was taken. Two significance thresholds are indicated, the more lenient 95% quantile of the maximum sequenceness of all permutations (lightly dotted line) and the maximum mean peak sequenceness across all permutations of all subjects (boldly dotted line). Sequenceness crossed the 95% permutation threshold in the post-learning resting state in minute 4 (backward 20 millisecond time lag). Note that sequenceness scores are negative for the latter, which would indicate a replay-suppression of these specific sequences.

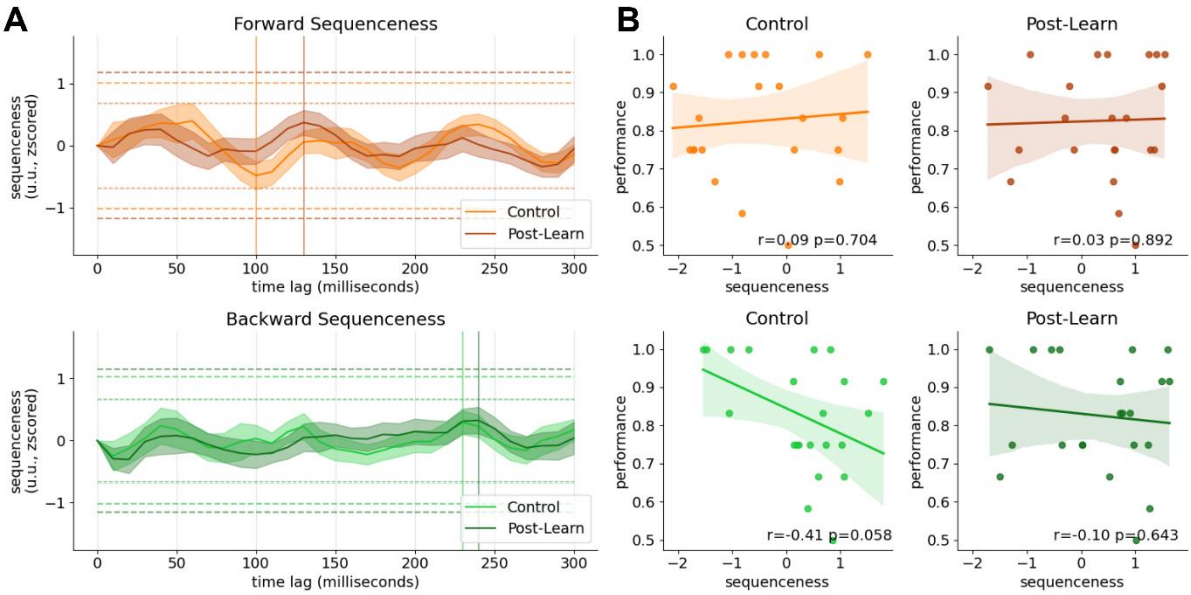

Supplement Figure 6 Sequenceness curves when not correcting for alpha oscillations. Alpha correction is usually applied to mitigate nuisance effects that are introduced by strong eyes-closed alpha by adding probability time lines in 100ms steps to the GLM (Y. Liu, Dolan, et al., 2021).

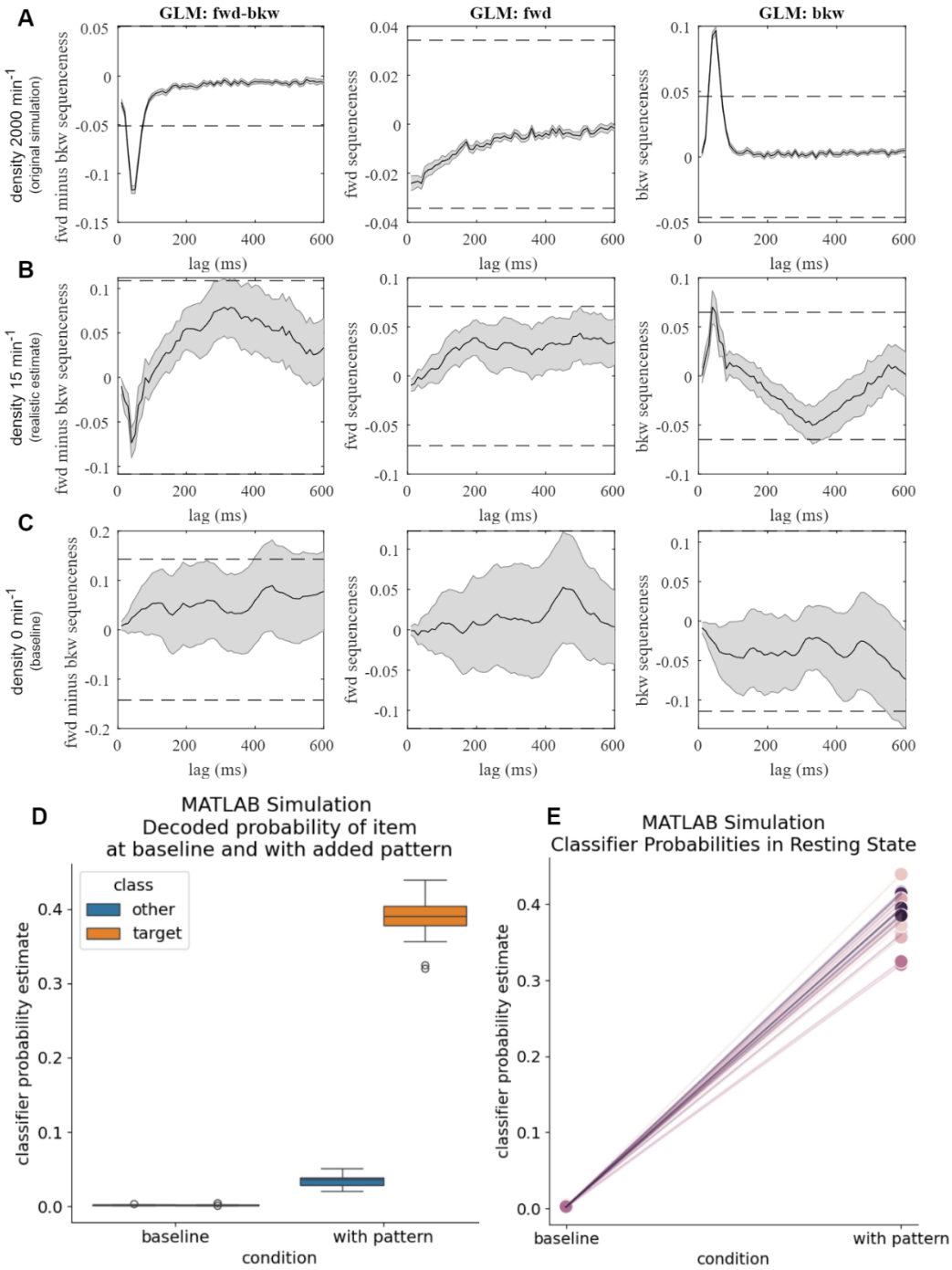

1215

Supplement Figure 7 A) Original TDLM (Y. Liu, Dolan, et al., 2021) simulation with a replay density of 2000 min^{-1}. B) Re-run of the code with realistic replay density of 15 min^{-1}. Using this density, significance thresholds are barely reached. C) Baseline sequenceness with no inserted sequences, some participants reach significance even in absence of replay, as can be seen by the confidence intervals D) Left: Time points at which no pattern has been inserted, both classes have a similar probability estimate at baseline. Right: At time points where the stimulus-specific pattern was added, the decoded probability estimate is significantly increased, cf. Figure 8. E) Probability estimates before and after insertion of the replay pattern, visualised as in Supplement Figure 2. It can be seen that the probability estimates at baseline are close to zero while increased by several orders of magnitude. Using synthetic data probably overestimates probability estimates of true events. Note that different from our simulation, the replay time lag has here been sampled from a gamma prior

with mean 40 milliseconds, such that the majority of events is simulated at 40 milliseconds, with some events getting assigned a lag of 30 or 50 milliseconds.

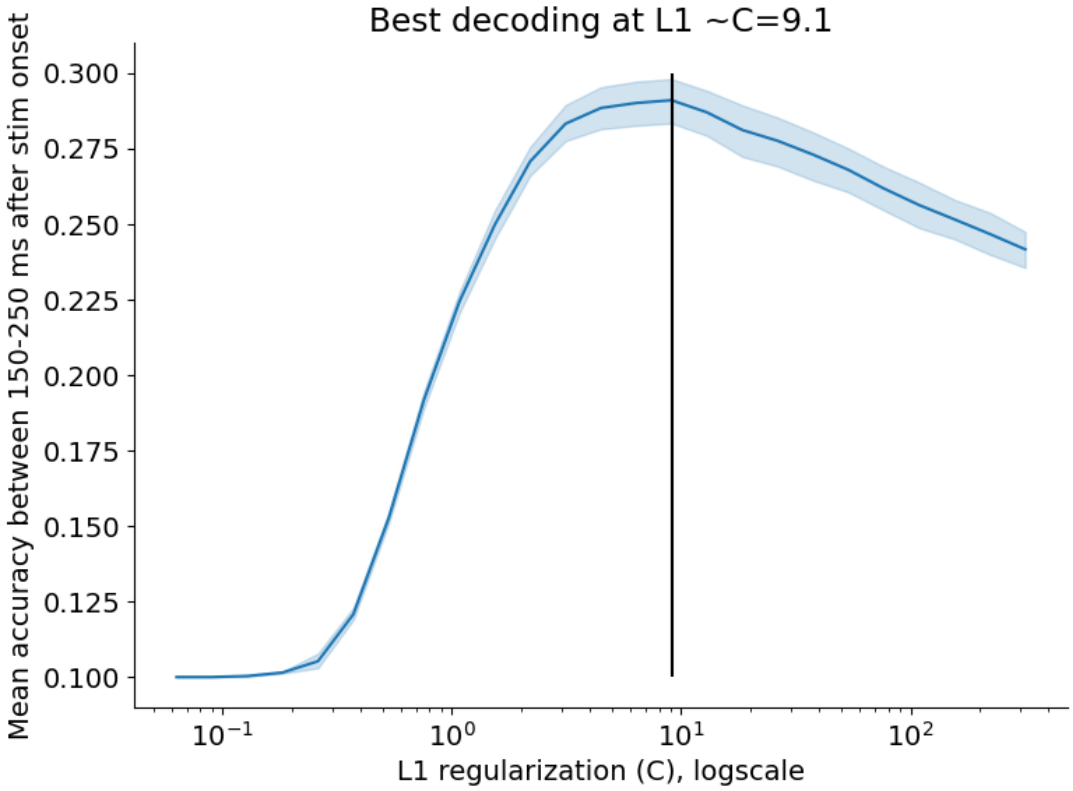

1216

Supplement Figure 8 *Cross-validation accuracy during the localizer across different regularization values. For each regularization value, a cross-validation was performed per participant as*

documented in the methods section, evaluated at 150 to 250 milliseconds after stimulus onset. The best regularization value was found around C=9.1

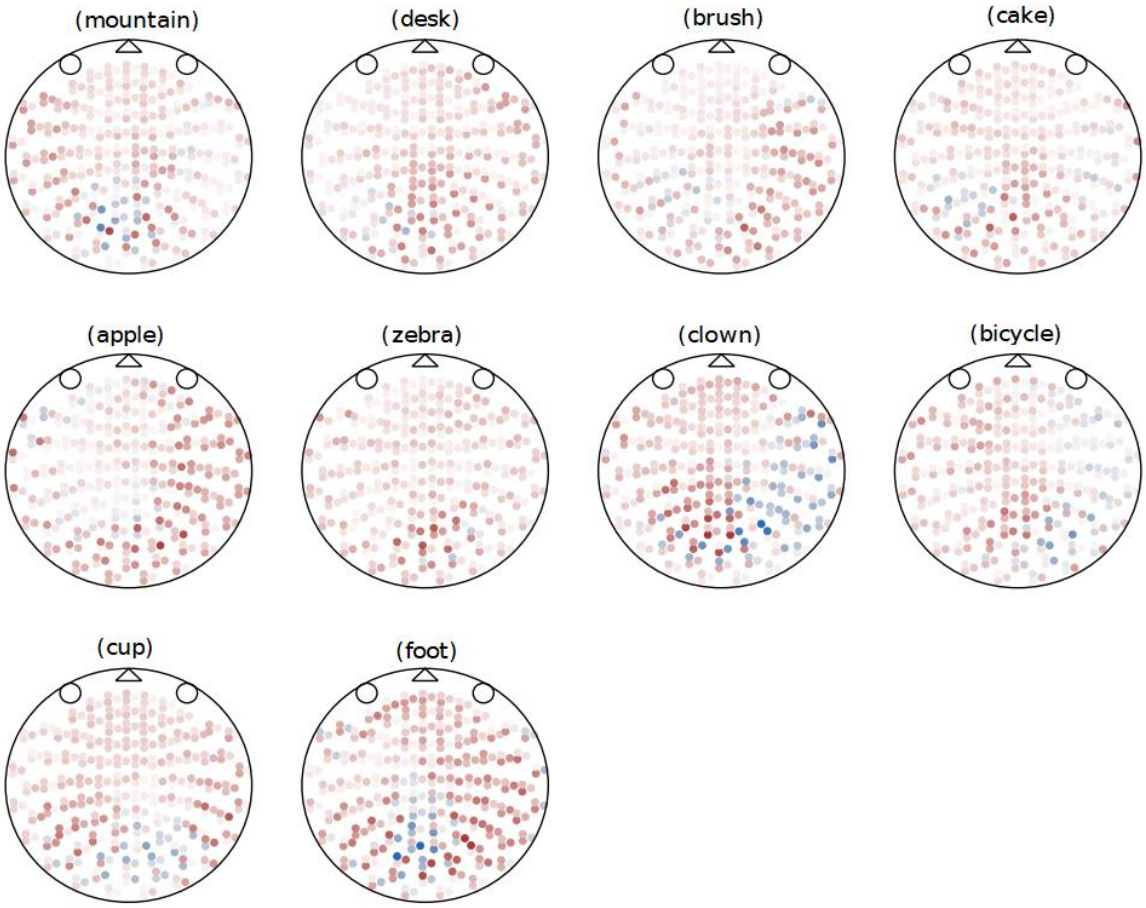

Supplement Figure 9 Visualization of the sensor patterns that were inserted into the resting state per class, averaged across all participants. Patterns were created on a per-participant-basis by taking the mean sensor value at the peak time point of decodability during the localizer of all trials of the specific class. From these patterns, the mean across all trials (the ERP) at the peak timepoint was subtracted, to remove activity related to general visual processing. Saturation indicates value magnitude (u.U.), red is positive sensor values, blue negative sensor value.

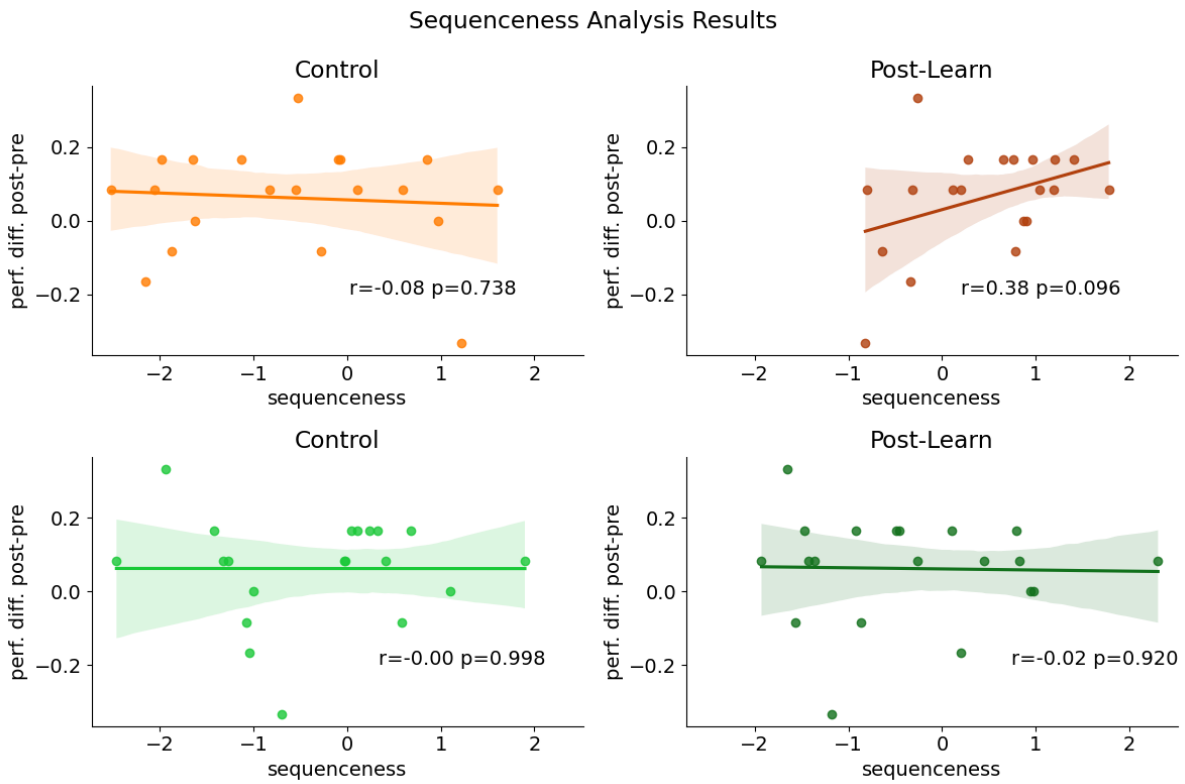

Supplement Figure 10 Individual participant's retrieval performance delta of the post-rest retrieval to the pre-rest retrieval relative to their sequenceness values at the peak mean sequenceness (indicated in A). Regression lines and 95% confidence intervals are fitted.